redin Revista Facultad de Ingeniería, Universidad de Antioquia, No.112, pp. 111-131, Jul-Sep 2024

Methods for evaluation of corrosion rate on magnesium alloys: a review

Métodos para evaluar la tasa de corrosión en aleaciones de magnesio: revisión

Juan Guillermo Castaño-González[1*], Luisa Fernanda Berrío[1], Félix Echeverría[1], Esteban Correa[2], Alejandro A. Zuleta[3]

[1]Centro de Investigación, Innovación y Desarrollo de Materiales CIDEMAT, Facultad de Ingeniería. Universidad de Antioquia. Código postal 050010. Calle 67 # 53-108, Medellín, Colombia.
[2]Grupo de Investigación Materiales con Impacto - MAT & MPAC, Facultad de Ingenierías, Universidad de Medellín. Código postal 050026. Carrera 87 # 30 – 65, Medellín, Colombia.
[3]Grupo de Investigación de Estudios en Diseño - GED, Facultad de Diseño Industrial, Universidad Pontificia Bolivariana. Código postal 050031. Circular 1 # 70-01, Medellín, Colombia.

CITE THIS ARTICLE AS:

J. G. Castaño-González, L. F. Berrío, F. Echeverría, E. Correa and A. A. Zuleta. "Methods for evaluation of corrosion rate on magnesium alloys: a review", *Revista Facultad de Ingeniería Universidad de Antioquia*, no. 112, pp. 111-131, Jul-Sep 2024. [Online]. Available: https://www.doi.org/10.17533/udea.redin.20240102

ARTICLE INFO:

Received: June 05, 2023
Accepted: January 30, 2024
Available online: January 30, 2024

KEYWORDS:

Magnesium; corrosion; mass loss; hydrogen evolution; potentiodynamic polarization

Magnesio; corrosión; pérdida de masa; evolución de hidrógeno; polarización potenciodinámica

ABSTRACT: The major drawback of some magnesium alloys is their low corrosion resistance. Therefore, the evaluation of corrosion resistance is a critical factor in developing new alloys and surface treatments. The techniques employed for the determination of corrosion rate include mass loss assessment, hydrogen evolution, potentiodynamic polarization, and electrochemical impedance spectroscopy (EIS). However, there are still difficulties in precisely estimating this parameter in Mg alloys. In this review, the reported applications, advantages, and disadvantages of the techniques mentioned above were analyzed. On the other hand, a large number of corrosion rate values reported for various Mg alloys in 3 different media (NaCl, Hanks´ solution and SBF), using mass loss, hydrogen evolution, and PP, were compared and analyzed. Generally, corrosion rates obtained from mass loss are higher than those obtained from hydrogen evolution. On the other hand, it is not possible to obtain correlations between corrosion rates obtained from PP and those obtained from mass loss and hydrogen evolution. Even more, dissimilar corrosion rate values are reported for the same alloy, implying that the measuring procedures are not well standardized.

RESUMEN: La mayor desventaja del uso de algunas aleaciones de magnesio es su baja resistencia a la corrosión. Por lo tanto, la evaluación de su resistencia a la corrosión es un factor crítico para el desarrollo de nuevas aleaciones y tratamientos superficiales. Las técnicas empleadas para determinar la tasa de corrosión incluyen determinaciones de pérdida de masa, evolución de hidrógeno, polarización potenciodinámica (PP) y espectroscopía de impedancia electroquímica (EIS), pero aún existen dificultades para la estimación precisa de este parámetro en aleaciones de magnesio. En esta revisión, se analizan las aplicaciones, ventajas y desventajas de las técnicas mencionadas antes. Además, se comparan y analizan un gran número de datos de tasa de corrosión reportados para varias aleaciones de Mg en 3 electrolitos diferentes (NaCl, solución de Hanks y SBF), usando pérdida de masa, evolución de hidrógeno y PP. Generalmente, las tasas de corrosión obtenidas mediante pérdida de masa son mayores que las obtenidas por evolución de hidrógeno. Por otro lado, no es posible establecer correlaciones entre tasas de corrosión obtenidas mediante PP y aquellas obtenidas por pérdida de masa y evolución de hidrógeno. Mas aún, se reportan tasas de corrosión muy diferentes para la misma aleación, lo que implica que los procedimientos de medición no están bien estandarizados.

1. Introduction

Because of excellent properties such as good thermal and electrical conductivity [1, 2], outstanding shock

* Corresponding author: Juan Guillermo Castaño-González
E-mail: juan.castano@udea.edu.co
ISSN 0120-6230
e-ISSN 2422-2844

absorption [3], high buffer capacity [3], and light weight [4], magnesium alloys have recently attracted significant interest and have great potential to serve in different industries like automotive [4, 5] and aerospace industry [4, 6], as well as in the area of biomaterials [3]. One major drawback of Mg is its active nature, making it an unstable material in almost any environment. Corrosion processes occur in the anodic areas, where metallic magnesium (Mg^0) passes to Mg^+ and then to Mg^{2+} to form Mg hydroxide. The corrosion mechanism of Mg alloys is similar in both the atmosphere (under a thin aqueous layer) and total immersion conditions. The only difference is the contribution of oxygen reduction, which is considered in atmospheric corrosion but can be ignored for immersion. The reactions in immersion conditions correspond to Equations (1) and (2) [7]:

$$Mg(s) \rightarrow Mg^{2+}(aq) + 2e^{-}(\text{anodic reaction}) \quad (1)$$

$$2\mathrm{H_2O(aq)} + 2e^{-} \rightarrow \mathrm{H_2}(g) + 2\mathrm{OH}^{-}(aq)(cathodic reaction) \quad (2)$$

The overall corrosion reaction can be expressed as Equation (3) or Equation (4):

$$\mathrm{Mg} + 2\mathrm{H_2O} \rightarrow \mathrm{Mg}^{2+} + 2(\mathrm{OH})^{-} + \mathrm{H_2} \quad (3)$$

$$\mathrm{Mg} + 2\mathrm{H_2O} \rightarrow \mathrm{Mg(OH)_2} + \mathrm{H_2} \quad (4)$$

For Mg alloys, corrosion is caused by the differences in potential due to the different phases present in the material microstructure [8]. Thus, the material quickly loses its properties due to the chemical reaction with the environment.

Different protection techniques against corrosion have been developed to solve these problems. The two most employed groups of techniques are as follows: the first one modifies the metal from the processing stage by developing advanced methods such as the compound extrusion process [9] or adding alloying elements that improve its corrosion resistance. Mg-Al, Mg-Zn, Mg-RE (Rare Earths), Mg-Ca, and Mg-Zn-Ca are some of the alloying systems developed with the aim of improving corrosion resistance. The second group consists of a series of surface treatments, such as coatings, in which a layer of a different material is deposited on the Mg substrate. Some surface treatment methods, including plating, electroless plating [10], micro-arc oxidation [11, 12], paints [13] and conversion coatings have been used to improve the corrosion resistance of Mg alloys. For the latter, the adhesion of the layer to the substrate is good, as well as the corrosion resistance, which is influenced by the thickness, composition, and morphology of the coating [14, 15].

To evaluate the performance of the abovementioned protection strategies, it is necessary to use methodologies that measure the degradation rate of the treated material in a given medium. Some techniques, such as weight loss and electrochemical tests, which have been used for such a purpose in other metals, have also been applied in Mg alloys. However, other techniques, such as the evolution of hydrogen and pH measurements have taken relevance in the scientific community. On the other hand, salt spray tests [16], although the high aggressiveness of the solutions used, can be used to evaluate the corrosion resistance of Mg alloys effectively. In this way, this review assesses the methodologies most widely applied for corrosion evaluation in Mg alloys: weight loss, hydrogen evolution, potentiodynamic polarization (PP), and electrochemical impedance spectroscopy (EIS), comparing the results obtained for each test and analyzing its advantages and limitations.

The data reviewed here only considered corrosion rate measurements on bare substrates. The most reported electrolytes are NaCl [17, 18], Simulated Body Fluids (SBF) [19, 20], and Hank´s solution (HS) [21, 22], and therefore, almost all papers reviewed used those solutions for testing the corrosion resistance of various Mg alloys. For a better analysis of the corrosion behavior from the data reported for mass loss, hydrogen evolution and PP, different figures are plotted for three groups of alloys: un-alloyed Mg, alloys without addition of RE, and alloys with addition of RE. On the other hand, the different colors of data points in these figures allow for differentiating the aggressive media or highlighting some particular alloys.

2. Mass loss

2.1 Basic description

The process consists of weighing the samples before and after immersion to obtain the weight difference caused by corrosion in an aggressive environment. To make the calculations of corrosion rate, different equations are employed. Equation (5) is extracted from the standard ASTM-G31 [23] for calculating the corrosion rate C_R in $\mathrm{mm \cdot y^{-1}}$:

$$C_R = \frac{8.76 * 10^4\ \mathrm{W}}{At\delta} \quad (5)$$

with W: mass loss (g), A: area of the original surface of each sample (cm^2), t: immersion time (h), $\boldsymbol{\delta}$: density of the sample $\left(\mathrm{g \cdot cm^{-3}}\right)$.
It has also been reported [24] the use of Equation (6) for measuring the weight loss corrosion rate:

$$C_R = \frac{W_o - W_1}{St} \quad (6)$$

with C_R: corrosion rate $\left(\mathrm{g \cdot cm^{-2} \cdot d^{-1}}\right)$, W_o: initial weight (g), W_1: weight after immersion (g), S: surface

area exposed to the test solution (cm^2), t: immersion time (days).

2.2 Reported applications

Mass loss is widely employed to study the corrosion of Mg alloys [25–71]. Figures 1 to 3 include corrosion rates from studies for different Mg alloys in NaCl, HS and SBF, using the mass loss technique. It is observed that most studies report results for immersion times up to 15 days ($\sim 83\%$) and, in most cases, the corrosion rates obtained are below 5 $\mathrm{mm \cdot y^{-1}}$ ($\sim$ 67%). For samples tested for more than two days, corrosion rates well above 5 $\mathrm{mm \cdot y^{-1}}$ are scarce, and in most of those cases, there is a clear explanation of the result (high contents of Zn, high contents of both Al and Zn in the same alloy, heat treatment in an AZ91D alloy) [32, 48–50]. On the other hand, low corrosion rates (below 1 $\mathrm{mm \cdot y^{-1}}$) have been reported for very diverse test conditions: various alloys, test media, and experimental times.

Figure 1 included corrosion rates at different times for unalloyed Mg. Error bars for the corrosion data plotted were included when this information was given in references. In NaCl and Hanks´s solution, the corrosion rate is high (above 20 $\mathrm{mm \cdot y^{-1}}$) in the first days [42, 44]. For all solutions (including SBF), the corrosion rates are relatively low at immersion times greater than two days [37, 41, 55]. The general trend, regardless of the solution used, is a marked decrease in the corrosion rate with time.

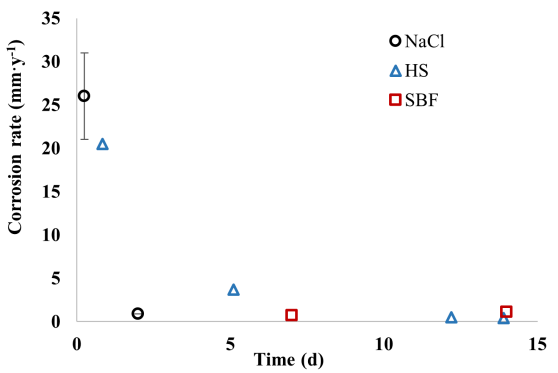

Figure 1 Corrosion rates vs. time for unalloyed Mg obtained by weight loss in different media [37, 41, 42, 44, 55]

In Figure 2a, the corrosion rates of Mg alloys without the addition of RE are plotted [26, 32, 33, 36–46, 48, 50, 52, 56, 69]. Error bars for the corrosion data plotted were included when this information was given in references. The trend for Mg alloys tested in HS solution is similar to that observed for un-alloyed Mg, with the corrosion rates being higher at low exposure times and lower at high exposure times. In the first days, the corrosion rates are higher if compared with un-alloyed Mg data (above 38 $\mathrm{mm \cdot y^{-1}}$ [46]). In NaCl, the corrosion rates tend to be lower than those reported in HS and SBF. In the case of the SBF solution, there is no clear trend. High corrosion rates were reported for different alloys even after 30 days. Almost all data at 30 days correspond to Mg-4Zn-0.2Ca with different additions of Al. For these contents of Zn and Ca, the corrosion rate increases to a great extent with the increment in Al. The authors found that the addition of Al from 3% to 10% produces intermetallic compounds in the grain boundaries and, hence, microgalvanic corrosion acceleration [48].

AZ91, AZ31, and Ca-alloys are the alloys with more data available among the Mg alloys without RE. Figure 2b included the same data as Figure 2a, but points for AZXX alloys are highlighted in different forms. For AZ91 alloys (square points), the corrosion rates are not very high at lower times, but the trend is that there is no decrease over time. These alloys are characterized by their good corrosion resistance. [26, 39–43]. However, for a heat-treated AZ91D alloy, the behavior is very different compared to other AZ91 and AZ91D data, showing a very high corrosion rate at seven days (unfilled square point). Mass loss experiments reveal how heat treatment of this AZ91D alloy increases the corrosion rate from 6.3 to 28 $\mathrm{mm \cdot y^{-1}}$ [32]. For AZ31 alloys, only one point (circular points) shows a very low corrosion rate after 14 days in NaCl [36]. For other AZ alloys (AZ61, AZ80 and AZ92), in general, the corrosion rates (diamond shape points) are low [36, 36, 44], except for an AZ80 alloy that exhibits a high corrosion rate (13.37 $\mathrm{mm \cdot y^{-1}}$) at five days in NaCl [38].

On the other hand, Figure 2c includes the same data as Figure 2a, but the points highlighted (square points) correspond to alloys with the addition of Ca and without Al [33, 45, 46, 48, 50]. The trend is similar to un-alloyed Mg, and relatively low corrosion rates (2.9 $\mathrm{mm \cdot y^{-1}}$) are reported for exposure times of up to 30 days [48]. The highest corrosion rates at low exposure times correspond to these alloys, reporting values close to 50 $\mathrm{mm \cdot y^{-1}}$, corresponding to an Mg-1.35Ca alloy [46]. However, for an extruded Mg-Li-Ca alloy, the corrosion rate is very low at a low exposure time. In this study, the extrusion of the alloy decreases the corrosion rate from 7 to 1.38 $\mathrm{mm \cdot y^{-1}}$ [33]. Other alloys included in Figure 2a are the following: Mg-0.2Mn-2Zn [40], MRI153M (Al-Zn-Mn-Ca-Sr alloy) [43], Mg-0.5Sr [45], and Mg-5Al-1Zn-1Sn [56]. All of them exhibit relatively low corrosion rates, even at times as long as 18 days, either in NaCl or HS.

In Figure 3, the corrosion rates of Mg alloys with the addition of RE are plotted [27, 39–44, 47, 49–51, 53, 54, 57, 70, 71]. Error bars for the corrosion data plotted were

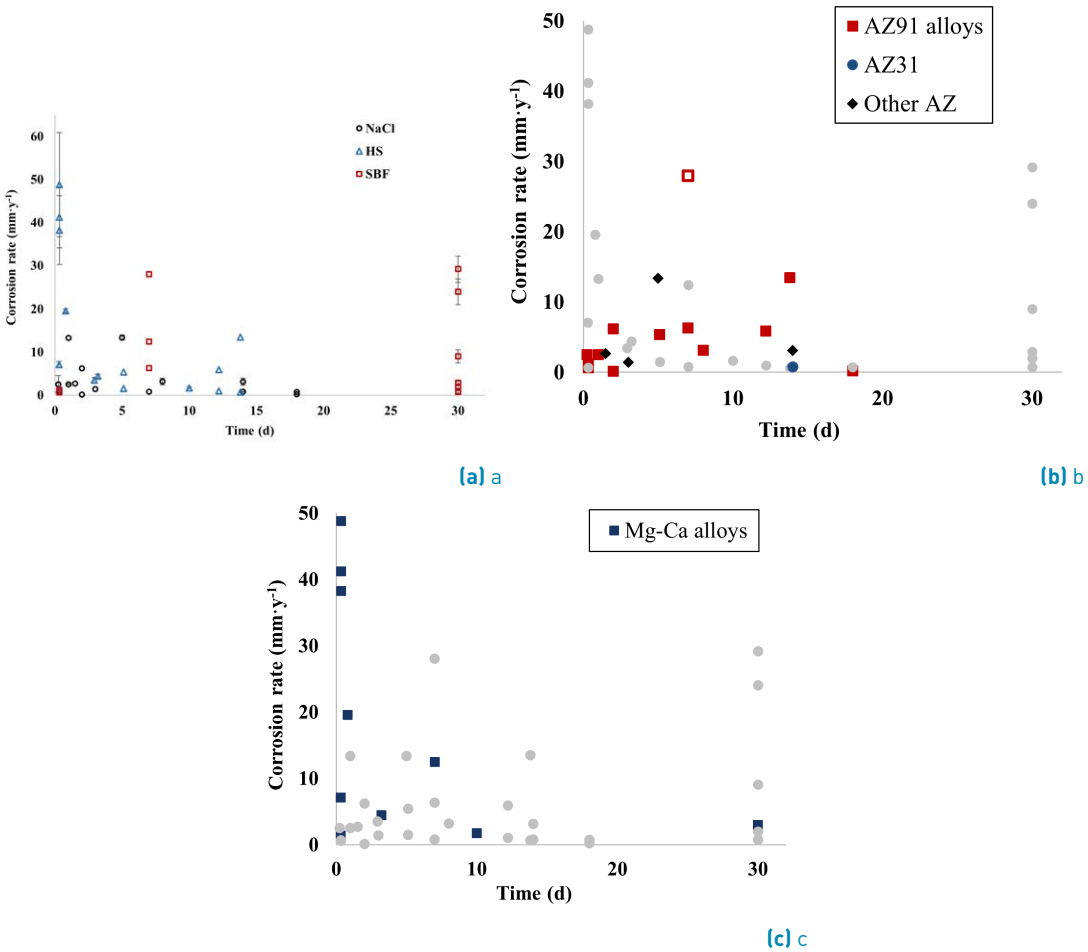

Figure 2 a) Corrosion rates vs. time for Mg alloys without RE obtained by weight loss in different media, b) The same data as in Figure 2a, but points corresponding to AZXX alloys are highlighted, c) The same data as in Figure 2a, but points corresponding to alloys with Ca and without Al are highlighted [26, 32, 33, 36–46, 48, 50, 52, 56, 69]

included when this information was given in references. The higher corrosion rates for this group of alloys are reported in NaCl, and correspond to 50 $\mathrm{mm} \cdot \mathrm{y}^{-1}$ for a Mg-10Y alloy and 30.9 $\mathrm{mm} \cdot \mathrm{y}^{-1}$ for a Mg-3Zn-0.3Ca-0.4La alloy. In this cast alloy, there is a strong galvanic process between cathodic second phases containing Y, Ca, or La and anodic Mg matrix, prompting the dissolution of the latter [49, 70]. For ZE41 alloy (Mg-Zn-Zr-RE), the reported corrosion rates are near 10 $\mathrm{mm} \cdot \mathrm{y}^{-1}$ at lower exposure times in NaCl [41, 42], and lower corrosion rates are reported at higher times, but in Hank´s solution [40]. For WE43 alloys (Mg-Zr-Y-Nd), only corrosion rates in SBF are reported [53, 57] and, in all cases, the values are lower than 3.5 $\mathrm{mm} \cdot \mathrm{y}^{-1}$. For a Mg-5.8Zn-0.7Mn-0.5Ca-0.4 Nd alloy, the corrosion rate in SBF is also near 11 $\mathrm{mm} \cdot \mathrm{y}^{-1}$ [50]. In the other cases, the corrosion rate is less than 5 in almost all the alloys and solutions reported. Despite the high variation in the composition of the alloys included, the general trend is a decrease in corrosion rate over time; however, a high corrosion rate is reported after 30-day immersion in HS for a Mg-Zr-0.35Zn2.85Nd-1.35Gd alloy. In this case, authors found intermetallic Mg12(Ndx,Gd1-x) phases precipitated in grain boundaries, as well as Zn-Zr phases inside the grains [71], which possibly cause important micro-galvanic effects. Besides studying the effect on the corrosion behavior of the addition of alloying elements [12, 14], the effect of other modifications of the material, such as heat treatment [31, 32] and mechanical deformation [33], on the corrosion rate have also been investigated using mass loss testing. As in many cases, corrosion of Mg alloys is related to galvanic effects between the second phases and the matrix, and both heat treatment and mechanical deformation induce changes in the alloy microstructure; these treatments may also modify the corrosion behavior of the alloy.

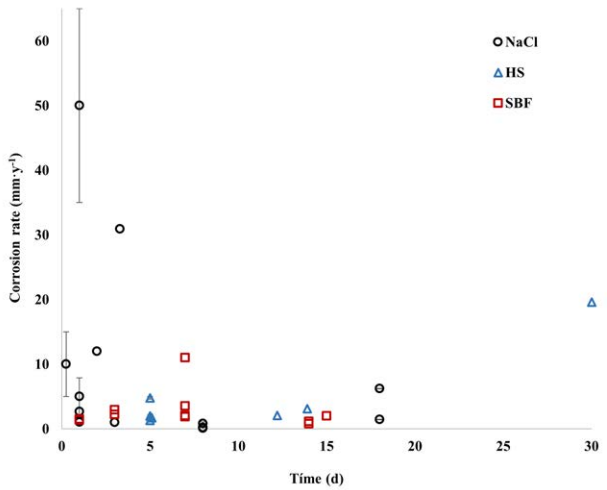

Figure 3 Corrosion rates vs. time for Mg alloys with RE obtained by weight loss in different media [27, 39–44, 47, 49–51, 53, 54, 57, 70, 71]

2.3 Advantages, limitations, and recommendations

As Mg corrodes, it goes from zero to 2^+ valence, so it passes to the solution in ionic form, and consequently, the sample loses mass [25]. However, Mg is not only dissolved, but it also forms solid byproducts, which are usually $Mg(OH)_2$. Therefore, in order to develop the measurement accurately, these corrosion products must be removed; in this sense, chromic acid is the most used compound for this purpose despite its environmental impact. Different authors reported the use of an aqueous mixture of chromic acid and silver nitrate [31, 41, 43, 47, 48]. An advantage of this cleaning solution is a negligible dissolution of the metal [42, 58–60]. Although more reports are found using this procedure at atmospheric temperature [39, 40], some experiments are also carried out at boiling temperature [26]. In a couple of cases, the cleaning procedure was carried out in an ultrasonic bath [44, 45]. Other authors reported the use of a boiling solution of CrO_3, with [32] and without $AgCrO_4$ [31, 52]. Despite the fact that it has been reported the absence of chromium compounds after the cleaning procedure of the Mg alloy surface, it is recommended, in any case, to avoid using these samples for further experimentation [42].

ASTM G-31 standard is widely accepted and employed to determine corrosion rates. ISO 8407 standard also specified procedures to remove corrosion products without significant removal of base metal for determination of the mass loss of different metals, including Mg. ASTM standard is particularly useful for in vitro tests, but has limitations in the interpretation of the degradation of magnesium alloys in vivo tests for longer periods. Some authors have proposed alternative methods for the determination of corrosion rates in hydrogen evolution tests [72] and in vivo tests [73]. However, there are no specific standards for these methods until now.

Although in most studies, replicate samples were used, only a few works report the weight loss values for each replicate [25], and others present the data in graphs with the respective uncertainties [31, 33, 36, 39, 42, 43, 45, 46, 53, 69, 70]. Despite the dispersion observed in some cases, the authors do not give any particular explanation. In the absence of further information, it can be considered that the method is highly sensible to any variation in sample processing [27]. Analysis of the same alloy by mass loss measurements, indicated significant differences depending on the processing of the alloy (as-cast, heat-treated, or mechanical processing) [32], which could be an indication of the sensitivity of the method. On the other hand, the ratio of solution volume to sample area employed for the immersion test has been reported to affect the results of a mass loss measurement [61]. These authors showed that for a ratio of 0.67, the corrosion rate was about 75% lower than when using a ratio of 6.7. However, according to those results, the effect of the solution volume/sample area ratio becomes insignificant when this ratio is high enough; in the case of that study above a 6.7 value, the corrosion rate is constant.

As one of the most important applications wanted for Mg alloys is in the field of biomaterials, it is very common to find studies where different simulated body fluid formulations are employed. As those solutions have different chemical compositions, it is unsurprising that different corrosion rates can be obtained for the various media. However, experiments in which all other conditions were maintained, except the solution employed are not very common. For example, for a Mg–Mn–Zn alloy, the corrosion rate in a Hank's solution was about twice the measured in a solution known as simulated blood plasma. The authors explained that the higher content of Cl^- ions in Hank's solution and the augmented amount of carbonate and phosphate ions in the other media were responsible for such a result [61]. Other studies report similar results [40]. However, uncertainty in the experimental setup precludes comparison. It is recommended that depending on the intended application of the biomaterial, both the solution volume/sample area ratio and the electrolyte should be carefully selected to ensure the immersion test results to be more representative of the actual environment [61]. In a complete review, different aspects of the experimental setups to be used for investigating the corrosion of Mg alloys for medical applications are discussed [62].

On the other hand, mass loss testing for the evaluation of

coated samples involves some difficulties [25]. Mass loss is particularly difficult to measure when material from the substrate becomes part of the coating during the coating process or is lost in the coating media. This is the case of conversion layers such as those obtained by anodization. In addition, coated Mg alloys might form a corrosion products layer underneath the coating surface, as it is well known. However, there are works in the literature reporting the use of mass loss techniques to measure corrosion rates in samples coated by different methods. Different situations are found in these works; either the authors did not remove the corrosion products and only accounted for the substrate material dissolved into the test electrolyte [63] or removed both the coating and corrosion products during the mass loss test [64, 65]. However, it is not very common that mass loss calculated from a mass loss test was much smaller than that obtained from a hydrogen evolution test [65]. Normally, the opposite is obtained. To avoid a possible artifact of the cleaning treatment in the CrO_3 solution in a study where Mg alloys were coated with a layer of MgF_2 [66], the authors carried out experiments on unexposed samples, in order to determine the amount of coating removed during this procedure. They found that the weight loss was just 0.1%. Due to the relatively high solubility of MgF_2 in chromic acid [67], this is an unsuspected result.

Some authors consider mass loss a standard and reliable method, but also pointed out some difficulties with this technique. It is not possible to know how the corrosion of the sample developed over time, and the value obtained is just a mean value for a given test period. On the other hand, the measurement could be inaccurate as it is not possible to be certain of the complete removal of the corrosion products without affecting the uncorroded material to some extent [68], or after long-term tests with severe corrosion of the samples, where it is very difficult to remove completely the corrosion products [74].

3. Hydrogen evolution

3.1 Basic description

As mentioned before, H_2 is one of the sub-products generated during the corrosion of Mg alloys, and because by each mole of H_2 released, one mole of Mg is oxidized, as Equation 3 shows, the amount of hydrogen evolved can be employed to measure the corrosion rate of Mg alloys [43] and is quite simple to measure [35, 42, 75, 76]. The sample is immersed in the corrosive solution, being NaCl in different concentrations, the solution most reported [33]. The necessary setup is shown in Figure 4, which is composed of a beaker, a graduated burette, and a funnel. The sample is placed in the middle of the beaker so that when H_2 is released, it goes directly from the funnel up to the burette, where a displacement of volume occurs [27]. Despite this experimental setup looking simple, there are some considerations to avoid erroneous results, both regarding the quality of the glassware and the design of the setup itself [77]. Regarding how the sample is located in the corrosive solution, i.e., vertically with both sides exposed or horizontally with the top side exposed, the results obtained for two different Mg alloys indicate no particular effect [75].

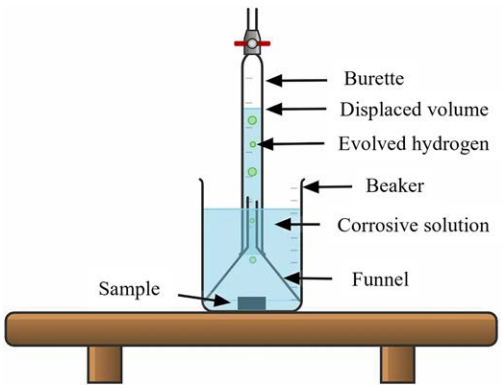

Figure 4 Setup diagram of the hydrogen evolution test

The evolution of gaseous hydrogen can be used to calculate the average corrosion rate of the material. The atmospheric pressure of the location where the experiment is carried out must be considered, and the following general expression can be used in order to obtain the mass change rate in $\mathrm{mg \cdot cm^{-2} \cdot d^{-1}}$ of Mg $(\Delta \mathrm{W})$ related to the rate of hydrogen evolution (VH) in $\mathrm{ml \cdot cm^{-2} \cdot d^{-1}}$ at any given atmospheric pressure (PATM) in atm. [77]:

$$\Delta W = 1.085 V_H / P_{ATM} \tag{7}$$

On the other hand, the corrosion rate of Mg can be calculated using the expression [59]:

$$P_H = 2.10 \Delta W \tag{8}$$

with P_H: average of the corrosion rate $\left(\mathrm{mm \cdot y^{-1}}\right)$.
Consequently, for standard conditions of the atmospheric pressure of 1 atm, the average corrosion rate in terms of the volume of hydrogen evolved in $\mathrm{ml \cdot cm^{-2} \cdot d^{-1}}$ will be [22, 59]:

$$P_H = 2.279 V_H \tag{9}$$

3.2 Reported applications

Hydrogen evolution tests have been used for different purposes: evaluation of coatings [58, 68, 78], analyses of the effect of some alloying [23, 79–81], and, in general, to assess the corrosion rate of Mg alloys [56, 79–99]. Figures 5 to 7 show some corrosion rate values obtained by hydrogen evolution in bare surfaces of different Mg alloys

in NaCl, HS, and SBF. Corrosion rates, when required, were calculated using Equations (7) to (9). According to the data included in Figures 5 to 7, most of the corrosion rate values ($\sim$ 93%) are below 12 $\mathrm{mm \cdot y^{-1}}$, and the experiments were carried out in most cases ($\sim$ 90%) by immersion of the samples for up to 20 days. It is observed that low corrosion rates (below 1 $\mathrm{mm \cdot y^{-1}}$) have been reported for very different experimental conditions: various alloy compositions, different electrolytes, and immersion times.

Figure 5 includes corrosion rates at different times for unalloyed Mg [21, 22, 40, 41, 45, 89–91]. Corrosion rates above 10 $\mathrm{mm \cdot y^{-1}}$ have been reported in HS at lower exposure times, and the highest value (17.1 $\mathrm{mm \cdot y^{-1}}$) [21] is consistent with the highest value reported for mass loss tests in HS. In NaCl and SBF corrosion rates reported are very low. The general trend is similar to that found in mass loss data: a decrease in the corrosion rate with time.

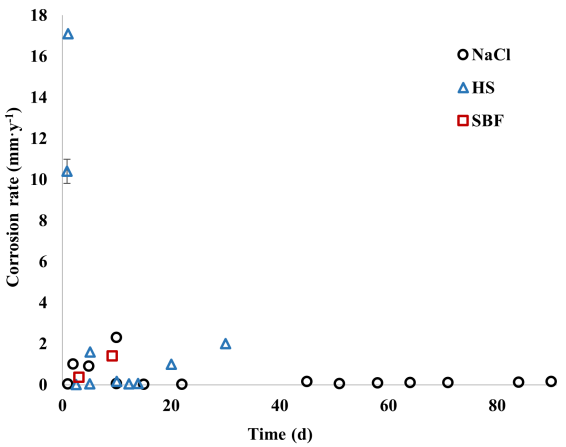

Figure 5 Corrosion rates vs. time for unalloyed Mg obtained by hydrogen evolution in different media [21, 22, 40, 41, 45, 89–91]

Figure 6a shows the data of corrosion rates of Mg alloys without the addition of RE [21, 22, 33, 36, 38–41, 43, 45, 46, 50, 56, 69, 79–81, 85–87, 89, 90, 92–98, 100, 101]. Error bars for the corrosion data plotted were included when this information was given in references. The general trends are similar for the three solutions considered: corrosion rates above 10 $\mathrm{mm \cdot y^{-1}}$ reported at first immersion times, but lower corrosion rates at higher times. However, particularly for the HS solution, the maximum values are lower than those reported for the other two solutions and very low corrosion rates are reported even at low immersion times. On the other hand, the highest corrosion rates in hydrogen evolution tests are reported in SBF (42.7 $\mathrm{mm \cdot y^{-1}}$ for an Mg-5Ca alloy) [22] and NaCl (36 $\mathrm{mm \cdot y^{-1}}$ for an AZ91 alloy) [89], while in mass loss tests the higher corrosion rates are reported in HS.

The alloys with more data available from hydrogen evolution tests are AZ91 and AZ31. Figure 6b includes the same data as Figure 6a, but points for AZ91 and AZ31 alloys are highlighted (square points for AZ91 and circular points for AZ31). The trends for both alloys are similar to the general trend observed for all data points, with lower corrosion rates at higher immersion times, but in the case of AZ91 is different from the trend observed for the same alloys in mass loss tests (Figure 2b). For AZ31 alloys, the corrosion rates are very low, even at immersion times between 28 and 48 days (below 0.16 $\mathrm{mm \cdot y^{-1}}$) [85, 96]. In the same figure, the corrosion rates corresponding to other AZXX alloys are also highlighted (diamond-shaped points) and include AZ61 [36] and AZ80 [38, 95] alloys. The values are lower than 5$\mathrm{mm \cdot y^{-1}}$ in most cases, similar to results observed in mass loss data (Figure 2b). There is only a report of a high corrosion rate (9.8 $\mathrm{mm \cdot y^{-1}}$ at 5 days in NaCl) for an AZ80 alloy, which is consistent with the corrosion rate for the same alloy in mass loss tests and similar media, reported by the same authors [38].

In Figure 6c, the highlighted square points correspond to alloys with an addition of Ca and without Al [33, 45, 46, 50, 79, 81, 89, 90, 92, 93, 99, 101]. At lower immersion times, both high and low corrosion rates were reported, although it must be considered the variability in aggressive solutions and chemical composition of alloys included in this group. As in the reports of mass loss, the highest corrosion rates at low exposure times correspond to an Mg-Ca alloy (42.7 $\mathrm{mm \cdot y^{-1}}$, reported for an Mg-5Ca alloy [87]).

Other alloys included in Figure 6a are the following: Mg-0.2Mn-2Zn [21, 40], Mg-1Zn [21], MRI153M (Al-Zn-Mn-Ca-Sr alloy) [43], Mg-0.5Sr [45], AM50 [80], Mg-5Al-1Zn-1Sn [56] and ZK30 [97]. Most of them exhibit relatively low corrosion rates, even at times as long as 30 days, either in NaCl or in HS. Only for an Mg-2Zn-0.2Mn alloy, a corrosion rate of 10 $\mathrm{mm \cdot y^{-1}}$ was reported at 5 days in NaCl [22].

In Figure 7, the corrosion rates of Mg alloys with the addition of RE are plotted [21, 22, 36, 40–42, 46, 49–51, 70, 88, 99] A decrease in corrosion rates with immersion time is observed, but this reduction is not as marked as in the previous cases. High corrosion rates are reported at times as long as 11 days (11.3 $\mathrm{mm \cdot y^{-1}}$ for an Mg-3Y alloy in HS) [99] and 18 days (7.73 $\mathrm{mm \cdot y^{-1}}$ for an MRI 202S alloy in NaCl) [42]. The highest corrosion rate for this group of alloys is 25.07 $\mathrm{mm \cdot y^{-1}}$ for an Mg-3Zn-0.3Ca-0.4La alloy in NaCl [49]; this behavior is very similar to that observed in the mass loss tests.

The data from mass loss and hydrogen evolution tests indicate that despite using very dissimilar experimental

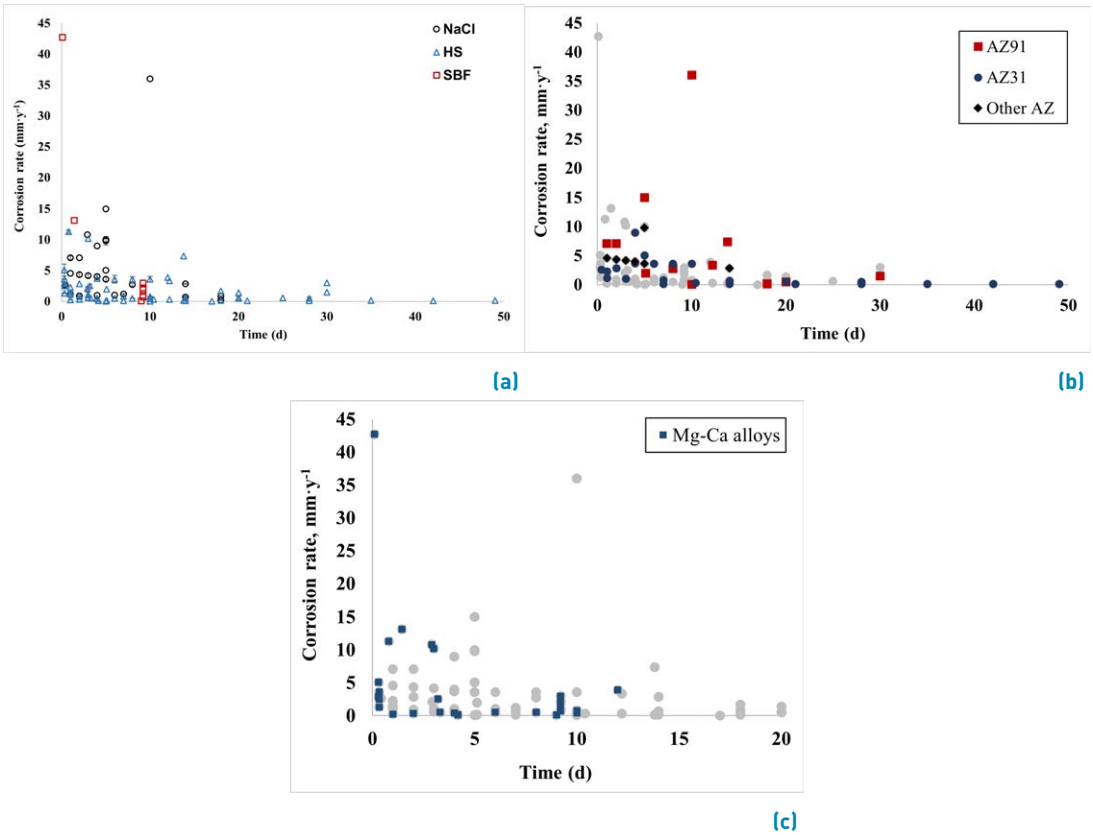

Figure 6 Corrosion rates vs. time for Mg alloys without RE obtained by hydrogen evolution in different media, b) The same data as in Figure 6a, but points corresponding to AZXX alloys are highlighted, c) The same data as in Figure 6a, but points corresponding to alloys with Ca and without Al are highlighted [21, 22, 36, 38–41, 43, 45, 46, 50, 56, 69, 79–81, 85–87, 89, 90, 92–98, 100, 101]

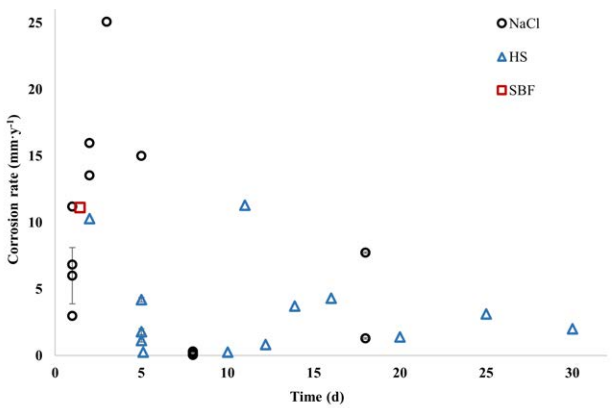

Figure 7 Corrosion rates vs. time for Mg alloys with RE obtained by hydrogen evolution in different media [21, 22, 36, 40–42, 46, 49–51, 70, 88, 89]

conditions, for Mg alloys, it is rare to obtain high corrosion rates for long immersion times. As the data included in Figures 2 to 7 correspond to bare surfaces of various Mg alloys, it might wrongly indicate that Mg alloys show a passivation behavior under different conditions. The above can be explained as during the corrosion process of Mg alloys, the pH of the electrolyte rises, and in most cases, the solution is not replaced; therefore, the sample-electrolyte system moves from the corrosion to the passivation zone as indicated in the respective potential-pH diagram [102].

In addition to the hydrogen evolved being an indicator of the corrosion kinetics of Mg alloys, , this result also indicates if a given alloy is suitable or not for use as implant material. This is due to the formation of gas pockets close to the implant, which negatively affects the healing process [21]. In this sense, hydrogen evolution tests are employed to establish if the gas production rate is below the maximum value the human body can handle ($0.01\ \mathrm{ml \cdot cm^{-2} \cdot day^{-1}}$) [21].

On the other hand, hydrogen evolution has been coupled with electrochemical methods to study Mg alloys' corrosion behavior both under open circuit conditions and when anodic polarization is applied [82]. Several setups of these characteristics have been reported, some very complex [83] and others more suitable for practical application in corrosion studies [72]. The latter work uses

an immersed container in which the H_2 gas is collected, and the H_2 volume is quantified using hydrostatic force principles [82]. On the other hand, a video system could be used to record the gas evolution in real time [72]. Some researchers employed a hydrogen evolution setup during electrochemical impedance measurements, looking to obtain a more accurate result. The use of hydrogen evolution measurements, together with weight loss tests, helped to a better interpretation of electrochemical results [85].

3.3 Advantages, limitations, and recommendations

One advantage of this test, if compared to the weight loss technique, is that the results are obtained during the immersion test itself. In contrast, loss mass requires the samples to be removed and processed at the desired immersion period, in order to calculate the corrosion rate at that time. By the hydrogen evolution test, the progress of corrosion can be easily followed just by looking at the hydrogen volume vs. immersion time graphs. By this means, it is possible to observe how an incubation period takes place at the beginning of the test [22, 40, 103, 104]. During that time, the corrosion rate is very low, and consequently, low amounts of hydrogen evolve; this period depends on the system alloy-electrolyte under testing and can vary from a few minutes to several days. Some researchers found that the incubation period for AZ41 alloy in NaCl solutions at various pH values, depends on both the NaCl concentration and the pH [104]. Other authors reported that also the duration of the incubation period is related to the alloy composition, and particularly, this period is affected by Zn and Mn contents [22, 105].

The incubation period obtained in the hydrogen evolution test is consistent with the incubation period found when monitoring the evolution of the open circuit potential (OCP); however, the incubation periods extracted from the OCP test are much shorter than those attained from a hydrogen evolution curve [106, 107]. On the other hand, the duration of the incubation period has been related to the corrosion rate of the alloy, so long incubation periods will lead to low corrosion rates and vice versa [105]. The incubation period is considered to disclose the breakdown of the partial protective film formed during sample preparation and the development of a less protective film, which is closely related to the system alloy-electrolyte [22, 40].

Generally, corrosion rates obtained from hydrogen evolution tests are lower than those obtained from mass loss tests [27, 56]. The explanation reported about this difference is that hydrogen could be absorbed by the Mg sample itself [27]. This was discussed in different works [22] for both pure Mg and various Mg alloys. In those studies, the authors calculated the amount of hydrogen dissolved in the metallic sample, assuming that the total hydrogen generated due to the corrosion process would be the equivalent of the weight loss value for a given sample, and plotted the hydrogen dissolved in the Mg alloy sample during the immersion test against the mass loss corrosion rate and obtained a linear relationship [106]. However, according to the literature, the solubility of hydrogen in Mg at room temperature is about $0.087\,\mathrm{cm^3 \cdot 100\,g^{-1}Mg}$ [107], and the maximum solubility in solid AZ91 alloy is about 24 ppm [108], the values calculated as hydrogen dissolved in the Mg alloy samples are well above these values. This disagreement was explained by other authors [109], noting that those calculations did not consider the amount of hydrogen that remains dissolved in the electrolyte. Other sources of error reported were the occurrence of corrosion mechanisms, which do not involve H_2 evolution, the variation of gas solubility with temperature, and the use of polymeric material in the measuring setup, which could be permeable to H_2 [77]. The latter two sources are either negligible or easily avoided. Regarding the problem with the H_2 dissolved in the electrolyte, one way to solve this problem is to pre-saturate the solution with H_2. This treatment is necessary if the amount of hydrogen dissolved is significant compared to the hydrogen evolved [110].

4. Potentiodynamic polarization

4.1 Basic description

This is a direct current electrochemical technique in which, using a three-electrode cell and a potentiostat, the cell current is measured as the potential of the working electrode is varied at a given rate [111]. As it is well known, by using the corrosion current extracted from PP curves, the corrosion rate of the alloy can be calculated. Equation (10) allows calculating the corrosion rate for Mg alloys [41, 112]:

$$P_i = 22.85 i_{\text{corr}} \tag{10}$$

with P_i: corrosion rate $\left(\mathrm{mm \cdot y^{-1}}\right)$, i_{corr}: corrosion current $\left(\mathrm{mA \cdot cm^{-2}}\right)$ obtained by means of Tafel extrapolation.

Mg has an atypical behavior, which is widely known as the Negative Difference Effect (NDE). Early reports of this anomalous effect were observed in neutral and acidic electrolytes [113]. When Mg and its alloys corrode, a strong evolution of hydrogen is also observed, and this reaction increases with anodic polarization. Other researchers stated that for Mg alloys, the electrochemical behavior is rather different from other metals: when the potential increases, hydrogen evolution also increases [8]. Although

similar phenomena can be observed in other metals (aluminum and ferrous alloys), the case of Mg is more complicated, as the hydrogen gas evolves both from the inside of the pits during a process of localized corrosion, as well as from the external surface, due to a cathodic reaction [114]. With the aim to explain this unusual behavior of Mg, several mechanisms have been proposed based on electrochemical reactions [8]. The definition of NDE given by these authors was more recently resumed in another work [115] as follows: if $\mathrm{I_{fp}}$ is the hydrogen evolution rate for an Mg electrode at the free corrosion potential and $\mathrm{I_{ap}}$ is the hydrogen evolution rate measured when applying a potential, the difference $\mathrm{I}_{fp} - \mathrm{I}_{ap}$ is found to be negative for Mg and increases and the potential is also increased. The model explaining NDE considers that corrosion of metallic Mg takes place first by the formation of Mg^{+} ions, which oxidize to $\mathrm{Mg^{2+}}$ by either an electrochemical or a chemical route. The occurrence of the univalent Mg^{+} ion had been reported several decades ago [116]. However, there are other issues leading to NDE. The variation of the active corrosion areas as the electrochemical potential also varies; additionally, it affects the accuracy of Tafel electrochemical methods for predicting the amount of Mg dissolved [117]. Other phenomena, such as particle loosening, have been widely reported during the corrosion of Mg alloys [8]. As the above problems are more critical during anodic polarization, the use of Tafel extrapolation of the cathodic branch appears to be a better approach. However, deviations between 48 and 96% from the corrosion rate values obtained from mass loss or hydrogen evolution techniques have been documented [115].

4.2 Reported applications

Figures 8 to 10 show different corrosion rates obtained by PP for different Mg alloys in NaCl, HS, and SBF. Error bars for the corrosion data plotted were included when this information was given in references. This method has been applied to reveal the effect of either surface modifications of the alloy [53, 118, 119], changes in the alloy bulk due to material manufacturing conditions [32, 52, 120–123], changes in electrolyte due to incorporation of corrosion inhibitors [124] and variations in the alloy chemical composition [48, 50, 90, 101, 125–127] or in Mg-based composite materials [128]. On the other hand, the polarization technique is widely reported for the evaluation of coatings [7, 13, 22, 46, 118, 120, 129, 130].

Figure 8 shows the corrosion rates reported for unalloyed Mg in NaCl [4, 91, 109] and SBF [55, 112, 125]. The corrosion rates in SBF are much higher, ranging from 7.33 and 35.56 $\mathrm{mm \cdot y^{-1}}$, and exhibit higher variability, whereas in NaCl, the corrosion rates are below 6.86 $\mathrm{mm \cdot y^{-1}}$

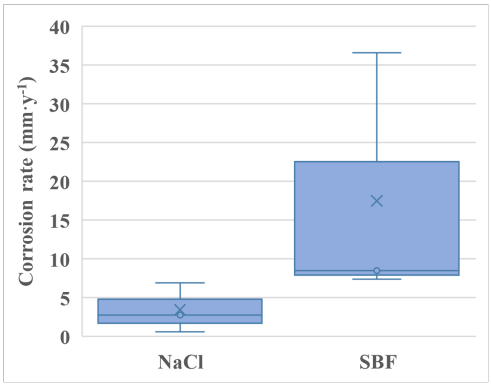

Figure 8 Corrosion rates for unalloyed Mg obtained by PP in different media [4, 55, 91, 109, 112, 125]

Figure 9 shows the corrosion rates for alloys without the addition of RE [32, 33, 38, 41, 44, 48, 50, 52, 56, 69, 76, 85–87, 90, 93–95, 98, 112, 118–120, 124, 125, 127–134]. According to Figure 9a, most of the corrosion rates are between 0.4 and 3.5 $\mathrm{mm \cdot y^{-1}}$. The median of the data for all the alloys included in this group is 0.87, which indicates that in many studies, the corrosion rates obtained correspond to low values (below 1 $\mathrm{mm \cdot y^{-1}}$). Very atypical values correspond to the higher corrosion rates found in Mg-0.2Ca-4Zn-10Al (28.33 $\mathrm{mm \cdot y^{-1}}$) [48], Mg-0.5Ca-1Mn-6Zn (25.27 $\mathrm{mm \cdot y^{-1}}$) [50] and Mg-0.2Ca-4Zn-7.5Al (22.85 $\mathrm{mm \cdot y^{-1}}$) [48] alloys, in all cases in SBF. The high corrosion rates in Mg-Ca-Zn-Al alloys obtained by PP by Homayun and Afshar [48] are similar to those obtained by mass loss. Figure 9b corroborates that higher corrosion values are reported in SBF, whereas lower corrosion values are obtained in HS. There is a great number of alloys included, and only some AZXX alloys are considered in different studies. In Figure 9c, corrosion rates for different AZXX alloys in different media are included. For AZ3X alloys, there is great variability in corrosion rates, ranging from 3.8 [87] to 9 $\mathrm{mm \cdot y^{-1}}$ in NaCl [131], whereas in HS, the corrosion rates are very lower, ranging from 0.16 [85] to 0.36 $\mathrm{mm \cdot y^{-1}}$ [95]. For AZ9X alloys, the corrosion rates are, in most cases, below 1 $\mathrm{mm \cdot y^{-1}}$ but exhibit some variability. The higher corrosion rates reported are 4.3 $\mathrm{mm \cdot y^{-1}}$ for AZ91 in NaCl [69], and 5.36 $\mathrm{mm \cdot y^{-1}}$ for AZ91D in SBF [128].

Figure 10 shows the corrosion rates obtained by PP for alloys with the addition of RE [41, 44, 49, 50, 53, 57, 70, 71, 135, 136]. Again, higher corrosion rates are reported in SBF. The only alloy with different reports is WE43 [53, 57, 126], and for this alloy, the corrosion rates have high variability, ranging from 3.5 to 12.7$\mathrm{mm \cdot y^{-1}}$. However, some authors found similar corrosion rates in mass loss and polarization tests (3.5 $\mathrm{mm \cdot y^{-1}}$) for WE43 alloy [57]. On the other

hand, the highest corrosion rate corresponds to an Mg-0.5Ca-1Mn-6Zn-0.4Nd alloy (26.2 $\mathrm{mm \cdot y^{-1}}$) [50]. High corrosion rates are also reported for this alloy in mass loss and hydrogen evolution test, by the same authors, but in both cases, are around 11 $\mathrm{mm \cdot y^{-1}}$. In this alloy, the addition of Nd does not seem to be beneficial.

Data in Figures 8 to 10 also show how corrosion rates obtained for this technique vary despite similar substrates and electrolytes being used in different studies (For example, for CP Mg, AZ31, AZ91, and WE43 alloys). Explanations of these variations include changes in the exact chemical composition of the electrolytes. Furthermore, this measuring method is sensible to differences in surface pretreatment and the time of immersion of the sample before starting the test. For this reason, researchers must provide detailed information on their test conditions. On the other hand, it must be considered that polarization measurements are instantaneous values of the corrosion rates, whereas mass loss and hydrogen evolution provide average values of corrosion rate in a given exposure time. The only similarity in Figures 8 to 10 is that the higher corrosion rates are obtained in SBF media.

4.3 Advantages, limitations, and recommendations

Despite the limitations due to NDE observed for Mg alloys, as discussed above, particularly when using PP for corrosion rate measurement, this technique is still widely employed. This is related in some cases to the ability of the technique to easily show the differences in corrosion behavior of either various alloys in the same electrolyte or the same material under various test conditions. Some researchers used this method to study the effect of alloy elements, surface treatments, heat treatments, mechanical treatments, etc., as well as variations in the test solution, such as the effect of various ions [100, 124–127, 129–137]. On the other hand, this technique produces instantaneous values of corrosion rates, which is both a limitation and an advantage: it cannot predict the long-term performance of the alloy in a given environment but provides a rapid evaluation and easy comparison of various material-environment systems.

5. Electrochemical impedance spectroscopy (EIS)

5.1 Basic description

EIS uses a small sinusoidal perturbation to study the reactions on the surface of a sample immersed in a given electrolyte, allowing a complete view of the corrosive phenomena on the surface of interest. The measurement system consists of a three-electrode cell, a potentiostat, and a frequency response analyzer [86, 111].

5.2 Reported applications

Several authors report the use of this technique to evaluate Mg alloys in corrosion studies [44, 47, 53, 70, 98, 112, 128, 138–143]. For example, in the corrosion process of a WE43 alloy, four stages are identified from EIS analysis [141]. In the first stage, occurs the oxidation of the matrix as evidenced by the release of hydrogen, during which $Mg(OH)_2$ is formed. The increase in thickness of the $Mg(OH)_2$ layer leads in the second stage to the formation of a MgO protective layer at the inner interface. For the third stage, the corrosion rate is reduced as the protective corrosion layer reaches its maximum, and a balance between the formation and dissolution rates of the corrosion layer is established. In this condition, pits are nucleated on the surface, which during the fourth stage growth to break the inner layer of MgO, induce further attack of the substrate.

One of the reasons for primarly using EIS for the study of corrosion mechanism rather than for corrosion rate measurement in Mg and its alloys has been clearly explained by Kirkland *et al.* [77]: In order to obtain corrosion currents from EIS data, applying the Stern–Geary equation, it is required to have the values of the cathodic and anodic Tafel slopes, which are difficult to measure for these materials as discussed above. For this reason, the data obtained from EIS in Mg materials are employed directly using the impedance of the system as indicative of the corrosion rate [70, 144]. With the use of EIS, researchers obtain the electrical properties of different films on the surface, and analysis of this information allows them to predict the role in the corrosion processes of the material [69, 98], as well as establish the oxygen diffusion and correlate this with corrosion and bioactivity in magnesium alloys used as biomaterials [145]. In addition, testing at various times is a powerful tool to follow the formation of corrosion product layers [133, 146]. Comparing Mg-Nd and Mg-Y alloys, some authors found that in both alloys, the diameter of the high-frequency capacitive loop decreases gradually as time increases, indicating that the protective nature of corrosion products films is affected by micro-galvanic corrosion of the alloys, and low-frequency inductive loops appear when localized corrosion starts [70]. Also, EIS analysis is widely employed to compare the corrosion performance of different Mg alloys [69, 139, 147], but only a few deducted corrosion rates from EIS data for this sort of materials [36, 141].

Some authors analyzed the correlation between the resistance data obtained from EIS and the corrosion rate

Figure 9 a) Corrosion rates for Mg alloys without RE obtained by PP in different media, b) Corrosion rates discriminated according to the electrolyte, c) Corrosion rates for 9XXX alloys [32, 33, 38, 41, 44, 48, 50, 52, 56, 69, 76, 85–87, 90, 93–95, 98, 112, 118–120, 124, 125, 127–134]

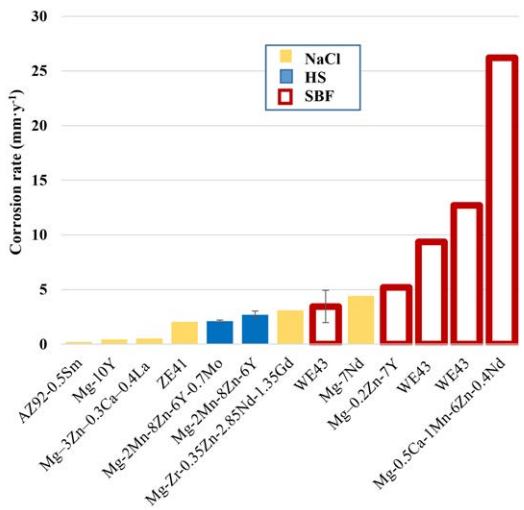

Figure 10 Corrosion rates for Mg alloys with RE obtained by PP in different media [41, 44, 49, 50, 53, 57, 70, 71, 135, 136]

of Mg alloys [146, 148], and found that to have accurate corrosion rate values from EIS data, a validation process should be performed. For instance, for a Mg-1Ca alloy in SBF, it was concluded that the charge transfer resistance showed the best correlation with the corrosion current measured by other techniques [148]. However, other authors studying pure Mg in a NaCl solution found that resistance at zero frequency is, for that system, the resistance value that better represents the corrosion resistance of the material, as compared with both mass loss and hydrogen evolution measurements [84]. On the other hand, the use of "Apparent Stern–Geary Coefficients", which are obtained empirically, allows for solving the difficulties in the determination of Tafel slopes for Mg and its alloys [86]. With these considerations, some authors have found similar corrosion rates in AZ31 (0.65 $\mathrm{mm \cdot y^{-1}}$ by mass loss, 0.67 $\mathrm{mm \cdot y^{-1}}$ by hydrogen evolution and 0.66 $\mathrm{mm \cdot y^{-1}}$ by EIS) and AZ61 alloys (3.23 $\mathrm{mm \cdot y^{-1}}$ by mass loss, 2.84 $\mathrm{mm \cdot y^{-1}}$ by hydrogen evolution and 3.58 $\mathrm{mm \cdot y^{-1}}$ by EIS) [36].

5.3 Advantages, limitations, and recommendations

Some of the more relevant advantages of EIS, are that little or no sample preparation is required. Measurements occur in real time, and it allows quantifying the formation of surface layers and their performance against corrosion in time. EIS also gives information on the kinetics of the reactions that occur during the test [41, 138, 141, 142] and could be a useful tool to determine the appearance of pitting [49, 70] and intergranular corrosion [149]. In contrast to polarization, the anodic and cathodic contributions cannot be identified in EIS tests. The biggest difficulty is the choice of an adequate equivalent circuit, which is crucial for proper analysis. A complex setup that, besides EIS experimentation, also allows monitoring Mg^{2+}, pH and H_2, has been reported for analyzing the behavior of 99.9% pure Mg samples in various electrolytes [143]. The authors also performed weight loss tests, and the results indicated good agreement between all the techniques except for some variation in trend for EIS. Similar experimental setups have been employed by other authors [84, 146, 148].

One important advantage of EIS compared to other techniques of measuring corrosion rates in this sort of material, such as mass loss and hydrogen evolution, is its higher resolution. On the other hand, limitations are related to the difficulty of obtaining accurate measurements due to the NDE observed in materials based on Mg, which consequently makes it difficult to

obtain accurate Tafel slopes, besides instability of Mg corrosion processes that cause dispersion in the EIS data. For these reasons, the use of EIS for the qualitative analysis of corrosion in Mg and its alloys is more frequently found in the literature, while quantitative measurements are scarce [86].

6. Comparative analysis

The general behavior of corrosion rates of magnesium and magnesium alloys has a similar trend in mass loss and hydrogen evolution tests: a decrease in corrosion rates with time.

Many corrosion tests are performed in NaCl solutions at room temperature for the evaluation of magnesium and magnesium alloys employed in the aerospace and automotive industries. Chlorides are very aggressive ions that actively participate in the corrosion process of metals. The advantage of NaCl solutions is that their concentration and pH do not change during the tests [150, 151].

Corrosion rates could be expected to be lower in HS and SBF than in NaCl due to the presence of phosphates and carbonates that promote the formation of protective or partially protective corrosion products, decreasing the corrosion rate [152]. However, this trend is not always observed. Depending on the test (mass loss or hydrogen evolution) and the type of alloy (unalloyed Mg, Mg alloys without RE, and alloys with RE), the corrosion rates reported for SBF and HS can be lower or higher if compared with corrosion rates reported in NaCl solutions. Tests in HS and SBF are performed at 37°C, and this temperature can somewhat accelerate the corrosion reactions compared to the room temperature in NaCl solutions. However, different corrosion product layers with different protective behavior can precipitate, and their composition will include different amounts of Ca^{2+}, carbonates, hydrocarbonates, and phosphates, depending on the solution employed [151, 152]. These differences in solutions, as well as the composition and microstructure of the different alloys included, determine their corrosion resistance.

For unalloyed magnesium, the corrosion rate decreases in mass loss and hydrogen evolution tests because of the formation of protective films on the surface and the absence of second phases that could originate micro-galvanic corrosion [150]. For these materials, the corrosion rates in SBF were always low, both in mass loss and hydrogen evolution tests. In mass loss tests, the higher corrosion rate corresponds to CP Mg in NaCl and low immersion time. The low corrosion rates found at low times in hydrogen evolution tests and NaCl are explained because, in this case, the material is high-purity (HP) Mg. In HP Mg, the impurities content (particularly Fe) is much lower than in CP Mg [153]. Therefore, its homogeneity is much higher.

In general, the corrosion rates reported for Mg alloys are higher than of unalloyed Mg, because Mg alloys contain, in addition of $\alpha - Mg$ phase observed in high purity alloys, one or more additional phases, and may contain other phases associated with impurity elements (Fe, Ni, Cu and Co) [153]. On the other hand, the grain size influences the corrosion resistance, and for the same alloy, the corrosion rate increases if the grains are coarser [43, 51].

In AZXX alloys, the higher corrosion rates reported in the mass loss and hydrogen test correspond to AZ91 and AZ80 alloys, while for AZ31 and AZ61 alloys, the corrosion rates are generally lower in any test or solution. Al and Zn have a moderate effect on the corrosion of magnesium alloys, because both increase the cathodic kinetics [152]. Several authors report that the higher the aluminum content (as is the case of AZ91 alloys), the greater the corrosion resistance due to the incorporation of Al in the bottom of the corrosion products layer, increasing its protective properties or the formation of a continuous network of β-phase (Mg17Al12), which hinders the corrosion propagation [153, 154]. However, the high corrosion rates reported for AZ91 in both mass loss and hydrogen evolution tests, even at 14 days, in tests performed in HS, was attributed to micro-galvanic acceleration of the corrosion [40], which indicates which that higher aluminum content does not always guarantee the formation of more protective phases or corrosion layers.

Mg-Ca alloys showed very high corrosion tests both in mass loss and hydrogen evolution tests. Ca is not beneficial for corrosion of Mg alloys, due to its reactivity. However, in alloys with low levels of Sr and Ca, corrosion rates reported in both tests are low, despite Sr having the ability to increase the corrosion rate of Mg dramatically [152]. Some researchers found that the addition of combined Sr and Ca in low levels improves the corrosion resistance of Mg alloys due to the formation of Ca/Sr-rich phases both in grain interior and grain boundaries, decreasing the difference in corrosion potential and hence the micro-galvanic effect [45]. In alloys with only Zn and Zn-Mn, the corrosion rates in both tests are always low, in agreement with the beneficial effect of the two elements [152]. Only for an Mg-2Zn-0.2Mn alloy, a corrosion rate near 10 mm·y-1 was reported in hydrogen evolution tests at 5 days in NaCl. The same authors found a corrosion rate of only 0.005 mm·y-1 at five days in HS for the same alloy. They claimed that in the HS the formation of more protective corrosion products significantly reduces the

micro-galvanic effects associated with the microstructure, whereas in NaCl, the microstructure has a great influence because the corrosion products are less protective [22]. However, the authors do not explain because the corrosion rate is significantly higher than other Mg-Zn-Mn evaluated in other studies.

Only for Mg alloys with RE is it clear that higher corrosion rates are reported in NaCl, both in mass loss and hydrogen evolution tests. According to the literature, the additions of some RE, such as Ce, La, Nd, Gd, Sm, and Y, in concentrations above their respective solubility limit are detrimental to the corrosion resistance of Mg alloys [152]. The highest corrosion rate in both tests corresponded to alloys with Mg-3Zn-0.3Ca-0.4La, evaluated in NaCl. In this case, researchers found a strong galvanic process between cathodic Mg-2Ca-6Mg-3Zn or Mg-Zn-La-Ca phases and anodic Mg matrix [49]. High corrosion rates are also reported in hydrogen evolution tests after 11 days for an Mg-3Y alloy in HS [99] and 18 days for an MRI 202S (0.38Zn-0.07Ca-0.41Zr-2Y-3.06Nd) alloy in NaCl [42], due probably to the high Y content. However, moderate corrosion rates are reported in Mg-10Gd alloys, and the authors claim that the high solubility of Gd in the $\alpha - \mathrm{Mg}$ matrix allows tailoring the corrosion rate in Mg-10Gd alloys due to the formation of Mg5Gd phases that reduce the galvanic effects between other noble phases, as GdH2, and $\alpha - \mathrm{Mg}$ matrix [47].

In Mg-Zn-Y-Mn alloys, the incorporation of low concentrations of Mo can improve the corrosion resistance due to the Mo influence in the grain refinement of the alloy and the higher electronegativity of Mo compared to other elements, which contributes to the stabilization of the grain boundaries [51]. On the other hand, in ZE41 alloys, the corrosion rates reported in the mass loss test are high at lower exposure times. Generally, these alloys contain approximately 1.53% of RE (1.05%Ce and 0.48La) and <0.002%Zr. In this case, the high contents of Ce and La, as well as the very low content of Zr, could explain the high corrosion rates, since low contents of Zr are also detrimental to corrosion [152].

Data from various studies [33, 36, 38–41, 43, 45, 49–51, 56, 69], where both weight loss and hydrogen evolution were employed to measure the corrosion rate of different Mg alloys, is presented in Figure 11. The solid line in the figure represents the condition for equality of the two measurements of the corrosion rates, and the dashed line corresponds to the slope (m) of the real data. According to the slope of the dashed line (m=0.65), generally, hydrogen evolution tests result in lower corrosion rates, in agreement with other comparative works [27]. Note that, in all cases, the results included in Figure 11 correspond to tests carried out under the same experimental conditions, i.e., equal materials, immersion solutions, and times.

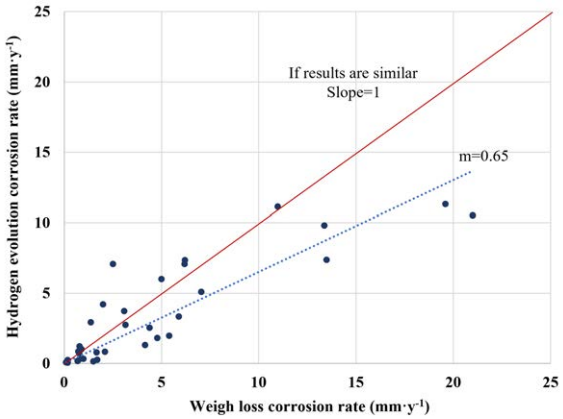

Figure 11 Comparison of the corrosion rates obtained by both hydrogen evolution and weight loss [33, 36, 38–41, 43, 45, 47, 49–51, 56]

Some possible explanations were given in section 3.3: absorption of hydrogen by the Mg sample itself, hydrogen that remains dissolved in the electrolyte, the occurrence of corrosion mechanisms that do not involve hydrogen evolution, the variation of gas solubility with temperature, and the use of polymeric material permeable to hydrogen in the measuring setup. Accounting all the possible sources of error, some authors considered that only 60% of the hydrogen generated during the corrosion of a Mg alloy is measured during a hydrogen evolution test [77]. This value is in close agreement with the value obtained from the graph in Figure 11 (0.65).

However, there are cases where the comparison of the corrosion rate of a Mg-Li-Ca alloy assessed by various methods reported the opposite: the corrosion rate obtained by weight loss was about 47% lower than that measured by hydrogen evolution. In this case, the differences are attributable to the corrosion mechanism in these alloys is pitting, which is difficult to evaluate through mass loss measurements [33]. On the other hand, the corrosion rates obtained from both mass loss and hydrogen evolution techniques were found to be very similar for most cases in Mg-Gd alloys, except for higher Gd content alloy (10 to 15%), where the corrosion rate calculated from the mass loss was between 17 and 25% lower than that obtained from hydrogen evolution [47]. The authors explained such a difference due to limitations in the cleaning procedure for the mass loss technique, together with errors in measuring the evolved gas amount [18]. At least, from the data analyzed here, the cases where weight loss tests generate lower corrosion rates than hydrogen evolution appear atypical.

The uncertainty or standard deviation between different

Table 1 Advantages and disadvantages of the different methods

Technique	Advantages	Disadvantages
Mass loss	Very simple. Does not require complex assemblies or equipment. Highly sensitive to sample processing. Useful to study the corrosion rate on different simulated body fluids solutions.	Measurements could not be accurate. Not recommended for coated Mg. Solutions for removal of corrosion products not friendly to the environment, such as CrO3 The samples must be removed and processed at the desired immersion period to calculate the corrosion rate.
Hydrogen evolution	Does not require complex assemblies or equipment. Suitable for bare and coated Mg. Useful to determine the incubation time before the corrosion initiation. The results are obtainedduring the immersion test itself.	Mg is a sensitive material to absorb hydrogen, which can affect the measurement of the hydrogen volume. Hydrogen evolution could be affected by the presence of $MgO/Mg(OH)_2$. Some H_2 dissolved in the electrolyte, affecting the calculations.
PP	Useful to determine the corrosion mechanism and the effect of time. Determination of corrosion rate in different media. Acceptable estimation of the corrosion current and corrosion potential from Tafel extrapolation of the curves. Wide utilization in corrosion studies of Mg, which allows comparison with other investigations.	The hydrogen evolution during the corrosion process affects the Tafel slope (NDE), which consequently makes it difficult to obtain accurate Tafel slopes. The rate of hydrogen evolution increases with increasing anodic polarization, which affects the corrosion rate value. The potential sweep rate affects the corrosion mechanisms.
EIS	No sample preparation is required. Measurements take place in real time. Determination of corrosion mechanisms. Informs about the porosity of the surface layer. Highly used for qualitative analysis and comparison.	The surface of the sample changes continuously, affecting the quantification. Determination of electrochemical parameters and corrosion mechanisms depends on the choice of an adequate equivalent circuit. Difficulty of obtaining accurate measurements due to the NDE.

techniques is variable depending on the alloys evaluated and the conditions of the tests. In different works, the corrosion rate evaluated from weight loss agrees within an error of $\sim \pm 10\%$ with the corrosion rate obtained from hydrogen evolution [115, 117]. In another report, the corrosion rate calculated by mass loss for unalloyed Mg had no significant difference with that obtained by hydrogen evolution ($p < 0.05$), if the volume loss is measured with a eudiometer, a real-time monitoring system developed in the last decade [74].

Regarding Polarization tests, the corrosion rates of Mg and Mg alloys in SBF are higher than in HS and NaCl. The high corrosion rates in Mg-Ca-Zn-Al alloys [48] are similar to those obtained by mass loss. On the other hand, some authors found similar corrosion rates in mass loss and polarization tests for WE43 alloy. Finally, the highest corrosion rate reported in polarization tests corresponds to an Mg-0.5Ca-1Mn-6Zn-0.4Nd alloy [50], and high corrosion rates are also reported for this alloy in mass loss and hydrogen evolution test, by the same author. The detrimental addition of Nd is corroborated by other authors [70], who found high corrosion rates in a Mg-7 Nd alloy in PP, mass loss, and hydrogen evolution tests.

However, when corrosion rates of Figures 8 to 10 are compared with data obtained by immersion tests (Figures 1 to 3) or hydrogen evolution (Figures 5 to 7), it is not possible to obtain any acceptable correlation. Two main reasons could explain these low correlations: First, the polarization technique might not be reliable for calculating the corrosion rate of Mg alloys, as the corrosion reactions involved may not comply with some fundamental requirements for the application of this technique (for example, there is not a single anodic or cathodic reaction) [41, 117]. The second reason deals with considering of similar immersion times for comparison [115]. This condition is not fulfilled for the data analyzed in this work, as generally, authors do not report the immersion times before PP tests. In addition, it must be considered that polarization measurements are instantaneous values, whilst hydrogen evolution and weight loss correspond to average values in time. This is evidenced when comparing data that despite using the same immersion times, there is still a large disagreement in the values obtained using the polarization method compared with the other two techniques [115].

The corrosion rates obtained from polarization curves exhibit higher uncertainties if compared with the corrosion rates obtained by mass loss or hydrogen evolution, showing typical deviations between 48 and 96%, approximately, being much larger than the precision of the measurement methods [115]. Different authors agreed that the most likely explanation is that part of the corrosion reaction is chemical rather than electrochemical [150]. Finally, for some authors, the corrosion rates determined by EIS have no significant difference from those obtained by mass loss and hydrogen evolution, if the resistance at zero frequency is considered for calculating the corrosion rate [84].

Finally, Table 1 summarizes the advantages and disadvantages of the revised methods.

7. Conclusions

All the techniques described in this review are complementary in the quest to understand and predict the corrosion behavior of Mg alloys, and the rest of metallic materials, considering that these techniques are an approximation of what can happen if the material is subjected to a certain environment.

Techniques that help visual analysis include immersion, weight loss, and evolution of hydrogen, but the corrosion values obtained from the two first methods are higher than the latter. All these techniques can be easily complemented; furthermore, weight loss and hydrogen evolution data can be obtained at the same time. On the other hand, it is not possible to obtain acceptable correlations between corrosion rates obtained by PP and those obtained by mass loss and hydrogen evolution.

From the literature, the sources of error when measuring corrosion rates for Mg alloys are identified for each one of the methods analyzed here. For weight loss and hydrogen evolution, error is mostly related to issues during the execution of the experiments, while in PP, the Mg corrosion processes might not comply with the theory supporting the method due to the NDE. This fact also causes limitations for obtaining corrosion rate measurements by EIS.

Very dissimilar corrosion rate values for the same Mg alloy were found, implying that the measuring procedures need to be better standardized and consequently a combination of techniques is always recommended.

8. Declaration of competing interest

We declare that we have no significant competing interests, including financial or non-financial, professional, or personal interests interfering with the full and objective presentation of the work described in this manuscript.

9. Funding

This project was funded by CODI-Universidad de Antioquia under Grant number PRG 14-1-06 and Centro de Investigación para el Desarrollo y la Innovación from the Universidad Pontificia Bolivariana under Gran number UPB-Innova Rad 747B-03/17-35.

10. Author contributions

J. G. Castaño: Data processing, results analysis. L. F. Berrío: Methodology, Investigation. F. Echeverría: Conceptualization. E. Correa: Methodology, results analysis. A. A. Zuleta: Results analysis, data processing.

11. Data availability statement

The authors confirm that the data supporting the findings of this study are available within the article [and/or] its supplementary materials.

References

[1] C. Wang, Z. Cui, H. Liu, Y. Chen, W. Diang, and S. Xiao, "Electrical and thermal conductivity in mg–5sn alloy at different aging status," *Materials & Design*, vol. 84, Nov. 05, 2015. [Online]. Available: https://doi.org/10.1016/j.matdes.2015.06.110

[2] B. L. Mordike and T. Ebert, "Magnesium: Properties — applications — potential," *Materials Science and Engineering: A*, vol. 302, no. 1, Apr. 15, 2001. [Online]. Available: https://doi.org/10.1016/S0921-5093(00)01351-4

[3] M. P. Staiger, A. M. Pietak, J. Huadmai, and G. Dias, "Magnesium and its alloys as orthopedic biomaterials: A review," *Biomaterials*, vol. 27, no. 9, Oct. 24, 2005. [Online]. Available: https://doi.org/10.1016/j.biomaterials.2005.10.003

[4] A. A. Luo, "8 - applications: aerospace, automotive and other structural applications of magnesium," *Fundamentals of Magnesium Alloy Metallurgy*, Mar. 27, 2014. [Online]. Available: https://doi.org/10.1533/9780857097293.266

[5] G. Cole, "18 - magnesium (mg) corrosion protection techniques in the automotive industry," *Corrosion Prevention of Magnesium Alloys*, Mar. 27, 2014. [Online]. Available: https://doi.org/10.1533/9780857098962.4.489

[6] R. M'Saoubi, D. Axinte, S. L. Soo, C. Nobel, H. Attia, G. Kappmeyer, S. Engin, and *et al.*, "High performance cutting of advanced aerospace alloys and composite materials," *CIRP Annals*, vol. 64, no. 2, Jul. 15, 2015. [Online]. Available: https://doi.org/10.1016/j.cirp.2015.05.002

[7] H. Liu, F. Cao, G.-L. Song, D. Zheng, Z. Shi, M. S. Dargusch, and A. Atrens, "Review of the atmospheric corrosion of magnesium alloys," *Journal of Materials Science & Technology*, vol. 35, no. 9, May. 09, 2019. [Online]. Available: https://doi.org/10.1016/j.jmst.2019.05.001

[8] G. L. Song and A. Atrens, "Corrosion mechanisms of magnesium alloys," *Advanced Engineering Materials*, vol. 1, no. 1, Feb. 02, 2000. [Online]. Available: https://doi.org/10.1002/(SICI)1527-2648(199909)1:1<11::AID-ADEM11>3.0.CO;2-N

[9] J. Liu, H. Hu, Y. Liu, D. Zhang, Z. Ou, and Y. Zhi, "Mechanical properties and wear-corrosion resistance of a new compound extrusion process for magnesium alloy az61," *Materials Testing*, vol. 62, no. 4, 2020. [Online]. Available: https://doi.org/10.3139/120.111476

[10] A. A. Zuleta, E. Correa, J. G. Castaño, F. Echeverría, A. Baron-Wiechec, P. Skeldon, and G. E. Thompson, "Study of the formation of alkaline electroless ni-p coating on magnesium and az31b magnesium alloy," *Surface and Coatings Technology*, vol. 321, Apr. 25, 2017. [Online]. Available: https://doi.org/10.1016/j.surfcoat.2017.04.059

[11] X.-J. Cui, X.-Z. Lin, C.-H. Liu, R.-S. Yang, X.-W. Zheng, and M. Gong, "Fabrication and corrosion resistance of a hydrophobic micro-arc oxidation coating on az31 mg alloy," *Corrosion Science*, vol. 90, Nov. 01, 2014. [Online]. Available: https://doi.org/10.1016/j.corsci.2014.10.041

[12] R. F. Zhang, S. F. Zhang, and S. W. Duo, "Influence of phytic acid concentration on coating properties obtained by mao treatment on magnesium alloys," *Applied Surface Science*, vol. 225, no. 18,

May. 04, 2009. [Online]. Available: https://doi.org/10.1016/j.apsusc.2009.04.145

[13] S. Mathieu, C. Rapin, J. Hazan, and P. Steinmetz, "Influence of phytic acid concentration on coating properties obtained by mao treatment on magnesium alloys," *Corrosion Science*, vol. 44, no. 12, May. 14, 2002. [Online]. Available: https://doi.org/10.1016/S0010-938X(02)00075-6

[14] M. Carboneras, L. A. Hernández-Alvarado, Y. E. Mireles, L. S. Hernández, M. García-Alonso, and M. Escudero, "Tratamientos químicos de conversión para la protección de magnesio biodegradable en aplicaciones temporales de reparación ósea," *Revista de Metalurgia*, vol. 46, no. 1, Ene-Feb. 2010. [Online]. Available: https://doi.org/10.3989/revmetalm.0944

[15] S. Hiromoto and A. Yamamoto, "Control of degradation rate of bioabsorbable magnesium by anodization and steam treatment," *Materials Science and Engineering: C*, vol. 30, no. 8, Jun. 08 2010. [Online]. Available: https://doi.org/10.1016/j.msec.2010.06.001

[16] Y. Wang, Z. Huang, Q. Yan, C. Liu, P. Liu, Y. Zhang, C. Guo, and *et al.*, "Corrosion behaviors and effects of corrosion products of plasma electrolytic oxidation coated az31 magnesium alloy under the salt spray corrosion test," *Applied Surface Science*, vol. 378, Apr. 06, 2016. [Online]. Available: https://doi.org/10.1016/j.apsusc.2016.04.011

[17] G. Wang, S. Ge, Y. Shen, H. Wang, Q. Dong, Q. Zhang, J. Gao, and *et al.*, "Study on the biodegradability and biocompatibility of we magnesium alloys," *Materials Science and Engineering: C*, vol. 32, no. 8, Jun. 06, 2012. [Online]. Available: https://doi.org/10.1016/j.msec.2012.05.050

[18] N. Hort, Y. Huang, D. Fechner, M. Störmer, C. Blawert, F. Witte, C. Vogt, and *et al.*, "Magnesium alloys as implant materials – principles of property design for mg–re alloys," *Acta Biomaterialia*, vol. 6, no. 5, Sep. 27, 2009. [Online]. Available: https://doi.org/10.1016/j.actbio.2009.09.010

[19] Y. K. Pan, C. Z. Chen, D. G. Wang, and Z. Q. Lin, "Preparation and bioactivity of micro-arc oxidized calcium phosphate coatings," *Materials Chemistry and Physics*, vol. 141, no. 2-3, Jul. 03, 2013. [Online]. Available: https://doi.org/10.1016/j.matchemphys.2013.06.013

[20] Y. Jang, B. Collins, J. Sankar, and Y. Yun, "Effect of biologically relevant ions on the corrosion products formed on alloy az31b: An improved understanding of magnesium corrosion," *Materials Chemistry and Physics*, vol. 9, no. 10, Mar. 25, 2013. [Online]. Available: https://doi.org/10.1016/j.actbio.2013.03.026

[21] G. Song, "Control of biodegradation of biocompatable magnesium alloys," *Corrosion Science*, vol. 49, no. 4, Feb. 06, 2007. [Online]. Available: https://doi.org/10.1016/j.corsci.2007.01.001

[22] N. I. Z. Abidin, D. Martin, and A. Atrens, "Corrosion of high purity mg, az91, ze41 and mg2zn0.2mn in hank's solution at room temperature," *Corrosion Science*, vol. 53, no. 3, Oct. 23, 2010. [Online]. Available: https://doi.org/10.1016/j.corsci.2010.10.008

[23] *Standard Guide for Laboratory Immersion Corrosion Testing of Metal*, ASTM G31-21, 2021. [Online]. Available: https://www.astm.org/g0031-21.html

[24] S. Guan, J. Hu, L. Wang, S. Zhu, H. Wang, J. Wang, W. Li, and *et al.*, "Mg alloys development and surface modification for biomedical application," in *Magnesium Alloys - Corrosion and Surface Treatments*, F. Czerwinski, Ed. Rijeka, Croatia: InTech, 2011. [Online]. Available: https://doi.org/10.5772/13187

[25] N. I. Z. Abidin, A. D. Forno, M. Bestetti, D. Martin, A. Beer, and A. Atrens, "Evaluation of coatings for mg alloys for biomedical applications," *Advanced Engineering Materials*, vol. 17, no. 1, Apr. 25, 2014. [Online]. Available: https://doi.org/10.1002/adem.201300516

[26] L.-J. Yang, Y.-H. Wei, L.-F. Hou, and D. Zhang, "Corrosion behaviour of die-cast az91d magnesium alloy in aqueous sulphate solutions," *Corrosion Science*, vol. 17, no. 1, Sep. 26, 2009. [Online]. Available: https://doi.org/10.1016/j.corsci.2009.09.020

[27] A. Atrens, G. L. Song, M. Liu, Z. Shi, F. Cao, and M. S. Dargusch, "Review of recent developments in the field of magnesium corrosion," *Advanced Engineering Materials*, vol. 17, no. 4, Jan. 07, 2015. [Online]. Available: https://doi.org/10.1002/adem.201400434

[28] C. Wang, L. Wu, F. Xue, R. Ma, I.-I. N. Etim, and *et al.*, "Electrochemical noise analysis on the pit corrosion susceptibility of biodegradable az31 magnesium alloy in four types of simulated body solutions," *Journal of Materials Science & Technology*, vol. 34, no. 10, Jan. 31, 2018. [Online]. Available: https://doi.org/10.1016/j.jmst.2018.01.015

[29] Q. Tian, J. A. Mendeza, L. Rivera-Castaneda, O. Mahmood, A. Showalter, E. Ang, and *et al.*, "Development of a novel loading device for studying magnesium degradation under compressive load for implant applications," *Materials Letters*, vol. 217, Dec. 30, 2017. [Online]. Available: https://doi.org/10.1016/j.matlet.2017.12.147

[30] X.-B. Chen, C. Li, and D. Xu, "Biodegradation of mg-14li alloy in simulated body fluid: A proof-of-concept study," *Bioactive Materials*, vol. 3, no. 1, Sep. 02, 2017. [Online]. Available: https://doi.org/10.1016/j.bioactmat.2017.08.002

[31] L. L. Shi, Y. Huang, L. Yang, F. Feyerabend, C. Mendis, and *et. al.*, "Mechanical properties and corrosion behavior of mg–gd–ca–zr alloys for medical applications," *Journal of the Mechanical Behavior of Biomedical Materials*, vol. 47, Mar. 14, 2015. [Online]. Available: https://doi.org/10.1016/j.jmbbm.2015.03.003

[32] W. Zhou, T. Shen, and N. N. Aung, "Effect of heat treatment on corrosion behaviour of magnesium alloy az91d in simulated body fluid," *Corrosion Science*, vol. 52, no. 3, Nov. 27, 2009. [Online]. Available: https://doi.org/10.1016/j.corsci.2009.11.030

[33] R.-C. Zeng, L. Sun, Y.-F. Zheng, H.-Z. Cui, and E.-H. Han, "Corrosion and characterisation of dual phase mg–li–ca alloy in hank's solution: The influence of microstructural features," *Corrosion Science*, vol. 79, Nov. 05, 2013. [Online]. Available: https://doi.org/10.1016/j.corsci.2013.10.028

[34] Y. Wang, M. Wei, J. Gao, J. Hu, and Y. Zhang, "Corrosion process of pure magnesium in simulated body fluid," *Materials Letters*, vol. 62, no. 14, Nov. 28, 2007. [Online]. Available: https://doi.org/10.1016/j.matlet.2007.11.045

[35] F. Witte, J. Fischer, J. Nellesen, H.-A. Crostack, V. Kaese, and *et. al.*, "In vitro and in vivo corrosion measurements of magnesium alloys," *Biomaterials*, vol. 27, no. 7, Aug. 24, 2005. [Online]. Available: https://doi.org/10.1016/j.biomaterials.2005.07.037

[36] S. Feliu and I. Llorente, "Corrosion product layers on magnesium alloys az31 and az61: Surface chemistry and protective ability," *Applied Surface Science*, vol. 347, May. 04, 2015. [Online]. Available: https://doi.org/10.1016/j.apsusc.2015.04.189

[37] Y. Dai, X.-H. Chen, T. Yan, A.-T. Tang, D. Zhao, and *et. al.*, "Improved corrosion resistance in az61 magnesium alloys induced by impurity reduction," *Acta Metallurgica Sinica (English Letters)*, vol. 33, May. 14, 2019. [Online]. Available: https://doi.org/10.1007/s40195-019-00914-2

[38] M. Liang, Y. M. C. Wu, J. Wang, M. Dong, B. Dong, and *et. al.*, "Influences of aggressive ions in human plasma on the corrosion behavior of az80 magnesium alloy," *Materials Science and Engineering: C*, vol. 119, Sep. 21, 2020. [Online]. Available: https://doi.org/10.1016/j.msec.2020.111521

[39] R. Arrabal, B. Mingo, A. Pardo, E. Matykina, M. Mohedano, and *et. al.*, "Role of alloyed nd in the microstructure and atmospheric corrosion of as-cast magnesium alloy az91," *Corrosion Science*, vol. 97, Apr. 20, 2015. [Online]. Available: https://doi.org/10.1016/j.corsci.2015.04.004

[40] N. I. Z. Abidin, A. D. Atrens, D. Martin, and A. Atrens, "Corrosion of high purity mg, mg2zn0.2mn, ze41 and az91 in hank's solution at 37 °c," *Corrosion Science*, vol. 53, no. 11, Jul. 03, 2011. [Online]. Available: https://doi.org/10.1016/j.corsci.2011.06.030

[41] M.-C. Zhao, M. Liu, G. L. Song, and A. Atrens, "Influence of microstructure on corrosion of as-cast ze41," *Advanced Engineering Materials*, vol. 10, no. 1-2, Feb. 12, 2008. [Online]. Available: https://doi.org/10.1002/adem.200700246

[42] G.-L. Song and Z. Shi, "Corrosion mechanism and evaluation of anodized magnesium alloys," *Corrosion Science*, vol. 85, Apr. 13, 2014. [Online]. Available: https://doi.org/10.1016/j.corsci.2014.04.008

[43] O. Gaon, G. Dror, O. Davidi, and A. Lugovskoy, "The effect of the

local microstructure of mri 201s magnesium alloy on its corrosion rate," *Corrosion Science*, vol. 93, Jan. 13, 2015. [Online]. Available: https://doi.org/10.1016/j.corsci.2015.01.018

[44] D. Wu, S. Yan, Z. Wang, Z. Zhang, R. Miao, and *et al.*, "Effect of samarium on microstructure and corrosion resistance of aged as-cast az92 magnesium alloy," *Journal of Rare Earths*, vol. 32, no. 7, Jul. 02, 2014. [Online]. Available: https://doi.org/10.1016/S1002-0721(14)60123-X

[45] M. Bornapour, M. Celikin, M. Cerruti, and M. Pekguleryuz, "Magnesium implant alloy with low levels of strontium and calcium: The third element effect and phase selection improve bio-corrosion resistance and mechanical performance," *Materials Science and Engineering: C*, vol. 35, Nov. 18, 2013. [Online]. Available: https://doi.org/10.1016/j.msec.2013.11.011

[46] R.-C. Zeng, W.-C. Qi, H.-Z. Cui, F. Zhang, S.-Q. Li, and *et al.*, "In vitro corrosion of as-extruded mg–ca alloys—the influence of ca concentration," *Corrosion Science*, vol. 96, Apr. 09, 2015. [Online]. Available: https://doi.org/10.1016/j.corsci.2015.03.018

[47] M. del R. Silva Campos, C. Blawert, C. L. Mendis, M. Mohedano, T. Zimmermann, and *et al.*, "Effect of heat treatment on the corrosion behavior of mg-10gd alloy in 0.5no. 84, Apr. 15, 2020. [Online]. Available: https://doi.org/10.3389/fmats.2020.00084

[48] B. Homayun and A. Afshar, "Microstructure, mechanical properties, corrosion behavior and cytotoxicity of mg–zn–al–ca alloys as biodegradable materials," *Journal of Alloys and Compounds*, vol. 607, Apr. 18, 2014. [Online]. Available: https://doi.org/10.1016/j.jallcom.2014.04.059

[49] Y. Du, X. Wang, D. Liu, W. Sun, and B. Jiang, "Corrosion behavior of a mg–zn–ca–la alloy in 3.5 wt% nacl solution," *Journal of Magnesium and Alloys*, vol. 10, no. 2, Sep. 24, 2020. [Online]. Available: https://doi.org/10.1016/j.jma.2020.08.004

[50] Y. Wang, Z. Liao, C. Song, and H. Zhang, "Influence of nd on microstructure and bio-corrosion rsistance of mg-zn-mn-ca alloy," *Rare Metal Materials and Engineering*, vol. 42, no. 4, Jul. 26, 2013. [Online]. Available: https://doi.org/10.1016/S1875-5372(13)60052-1

[51] L. Zhang, Y. Zhang, J. Zhang, R. Zhao, and J. Zhang, "Effect of alloyed mo on mechanical properties, biocorrosion and cytocompatibility of as-cast mg–zn–y–mn alloys," *Acta Metallurgica Sinica (English Letters)*, vol. 33, Jan. 07, 2020. [Online]. Available: https://doi.org/10.1007/s40195-019-00995-z

[52] Y. Song, E. H. Han, D. Shan, C. D. Yim, and B. S. You, "The role of second phases in the corrosion behavior of mg–5zn alloy," *Corrosion Science*, vol. 60, Mar. 31, 2012. [Online]. Available: https://doi.org/10.1016/j.corsci.2012.03.030

[53] W. Jin, G. Wu, H. Feng, W. Wang, and X. Zhang, "Improvement of corrosion resistance and biocompatibility of rare-earth we43 magnesium alloy by neodymium self-ion implantation," *Corrosion Science*, vol. 94, Feb. 04, 2015. [Online]. Available: https://doi.org/10.1016/j.corsci.2015.01.049

[54] Y. Gui, Q. Li, and J. Chen, "International journal of electrochemical science," *Corrosion Science*, vol. 14, no. 2, Jun. 26, 2023. [Online]. Available: https://doi.org/10.20964/2019.02.25

[55] X. Zhan, S.-D. Cui, L. Zhou, J.-B. Lian, J. He, and *et al.*, "Preparation and characterization of calcium phosphate containing coating on plasma electrolytic oxidized magnesium and its corrosion behavior in simulated body fluids," *Journal of Alloys and Compounds*, vol. 896, Nov. 30, 2021. [Online]. Available: https://doi.org/10.1016/j.jallcom.2021.163042

[56] Y. Ma, H. Xiong, and B. Chen, "Effect of heat treatment on microstructure and corrosion behavior of mg-5al-1zn-1sn magnesium alloy," *Corrosion Science*, vol. 191, Aug. 12, 2021. [Online]. Available: https://doi.org/10.1016/j.corsci.2021.109759

[57] J. Li, J. Li, Q. Li, H. Zhou, G. Wang, and *et al.*, "Titania-zinc phosphate/nanocrystalline zinc composite coatings for corrosion protection of biomedical we43 magnesium alloy," *Surface and Coatings Technology*, vol. 410, Feb. 04, 2021. [Online]. Available: https://doi.org/10.1016/j.surfcoat.2021.126940

[58] Z. Shi and A. Atrens, "An innovative specimen configuration for the study of mg corrosion," *Corrosion Science*, vol. 53, no. 1, Sep. 16, 2010. [Online]. Available: https://doi.org/10.1016/j.corsci.2010.09.016

[59] M. C. Zhao, M. Liu, G. Song, and A. Atrens, "Influence of the ß-phase morphology on the corrosion of the mg alloy az91," *Corrosion Science*, vol. 50, no. 7, Apr. 26, 2008. [Online]. Available: https://doi.org/10.1016/j.corsci.2008.04.010

[60] G. Song, A. L. Bowles, and D. H. StJohn, "Corrosion resistance of aged die cast magnesium alloy az91d," *Materials Science and Engineering: A*, vol. 366, no. 1, Nov. 14, 2003. [Online]. Available: https://doi.org/10.1016/j.msea.2003.08.060

[61] L. Yang and E. Zhang, "Biocorrosion behavior of magnesium alloy in different simulated fluids for biomedical application," *Materials Science and Engineering: C*, vol. 29, no. 5, Jan. 22, 2009. [Online]. Available: https://doi.org/10.1016/j.msec.2009.01.014

[62] J. Gonzalez, R. Q. Hou, E. P. Nidadavolu, R. Willumeit-Römer, and F. Feyerabend, "Magnesium degradation under physiological conditions – best practice," *Bioactive Materials*, vol. 3, no. 2, Feb. 14, 2018. [Online]. Available: https://doi.org/10.1016/j.bioactmat.2018.01.003

[63] L. Bai, G. Kou, K. Zhao, G. Chen, and F. Yan, "Effect of in-situ micro-arc oxidation coating on the galvanic corrosion of az31mg coupled to aluminum alloys," *Journal of Alloys and Compounds*, vol. 775, Oct. 15, 2018. [Online]. Available: https://doi.org/10.1016/j.jallcom.2018.10.154

[64] Y. Ren, E. Babaie, B. Lin, and S. B. Bhaduri, "Microwave-assisted magnesium phosphate coating on the az31 magnesium alloy," *Biomedical Materials*, vol. 12, no. 4, Aug. 2017. [Online]. Available: https://doi.org/10.1088/1748-605X/aa78c0

[65] Y. Reyes, A. Durán, and Y. Castro, "Glass-like cerium sol-gel coatings on az31b magnesium alloy for controlling the biodegradation of temporary implants," *Surface and Coatings Technology*, vol. 307, no. Part A, Sep. 26, 2016. [Online]. Available: https://doi.org/10.1016/j.surfcoat.2016.09.056

[66] J.-M. Seitz, K. Collier, E. Wulf, D. Bormann, and F.-W. Bach, "Comparison of the corrosion behavior of coated and uncoated magnesium alloys in an in vitro corrosion environment," *Advanced Engineering Materials*, vol. 13, no. 9, May. 23, 2011. [Online]. Available: https://doi.org/10.1002/adem.201080144

[67] P. Makkar, H. J. Kang, A. R. Padalhin, I. Park, B.-G. Moon, and *et al.*, "Development and properties of duplex mgf^2/pcl coatings on biodegradable magnesium alloy for biomedical applications," *PLoS One*, vol. 13, no. 4, Apr. 02, 2018. [Online]. Available: https://doi.org/10.1371/journal.pone.0193927

[68] G. Song, "Recent progress in corrosion and protection of magnesium alloys," *Advanced Engineering Materials*, vol. 7, no. 7, Jul. 29, 2005. [Online]. Available: https://doi.org/10.1002/adem.200500013

[69] W. Qiu, Y. Li, G. Huang, J. Chen, Y. Ren, and *et al.*, "Corrosion behavior of as-cast az91 magnesium alloy with vn particle additions in nacl solution," *Transactions of Nonferrous Metals Society of China*, vol. 33, no. 5, Jun. 12, 2023. [Online]. Available: https://doi.org/10.1016/S1003-6326(23)66191-6

[70] H. Zhang, Y. Zhao, J. Liu, J. Xu, D. Guo, and *et al.*, "Impact of rare earth elements on micro-galvanic corrosion in magnesium alloys: A comparative study of mg-nd and mg-y binary alloys," *International Journal of Electrochemical Science*, vol. 18, no. 6, Apr. 20, 2023. [Online]. Available: https://doi.org/10.1016/j.ijoes.2023.100160

[71] L. A. Rojas-Flórez, H. A. Briceño-Urbina, and C. A. Hernández-Barrios, "Síntesis y evaluación de recubrimientos base fl uoruro empleando fuentes alternativas al hf sobre la aleación elektron 21 para la fabricación de implantes ortopédicos biodegradables," *Revista ION*, vol. 28, no. 2, Jul-Dec. 2015. [Online]. Available: https://doi.org/10.18273/revion.v28n2-2015001

[72] M. Curioni, "The behaviour of magnesium during free corrosion and potentiodynamic polarization investigated by real-time hydrogen measurement and optical imaging," *Electrochimica Acta*, vol. 120, Jan. 03, 2014. [Online]. Available: https://doi.org/10.1016/j.electacta.2013.12.109

[73] E. P. S. Nidadavolu, F. Feyerabend, T. Ebel, R. Willumeit-Romer, and M. Dahms, "On the determination of magnesium degradation

rates under physiological conditions," *Materials*, vol. 9, no. 8, Jul. 28, 2016. [Online]. Available: https://doi.org/10.3390/ma9080627

[74] L. Liu, K. Gebresellasie, B. Collins, H. Zhang, Z. Xu, and *et al.*, "Degradation rates of pure zinc, magnesium, and magnesium alloys measured by volume loss, mass loss, and hydrogen evolution," *Applied Sciences*, vol. 8, no. 9, Aug. 25, 2018. [Online]. Available: https://doi.org/10.3390/app8091459

[75] A. Samaniego, I.Llorente, and S. Feliu-Jr, "Combined effect of composition and surface condition on corrosion behaviour of magnesium alloys az31 and az61," *Corrosion Science*, vol. 68, Nov. 14, 2012. [Online]. Available: https://doi.org/10.1016/j.corsci.2012.10.034

[76] H. R. Bakhsheshi-Rad, E. Hamzah, M. Daroonparvar, R. Ebrahimi-Kahrizsangi, and M. Medraj, "In-vitro corrosion inhibition mechanism of fluorine-doped hydroxyapatite and brushite coated mg–ca alloys for biomedical applications," *Ceramics International*, vol. 40, no. 6, Jan. 07, 2014. [Online]. Available: https://doi.org/10.1016/j.ceramint.2013.12.147

[77] N. T. Kirkland, N. Birbilis, and M. P. Staiger, "Assessing the corrosion of biodegradable magnesium implants: A critical review of current methodologies and their limitations," *Acta Biomaterialia*, vol. 8, no. 3, Nov. 18, 2011. [Online]. Available: https://doi.org/10.1016/j.actbio.2011.11.014

[78] G. S. Frankel and A. S. ad N. Birbilis, "Evolution of hydrogen at dissolving magnesium surfaces," *Corrosion Science*, vol. 70, Jan. 16, 2013. [Online]. Available: https://doi.org/10.1016/j.corsci.2013.01.017

[79] C. L. Liu, Y. J. Wang, R. C. Zeng, X. M. Zhang, W. J. Huang, and *et al.*, "In vitro corrosion degradation behaviour of mg–ca alloy in the presence of albumin," *Corrosion Science*, vol. 52, no. 10, Jun. 15, 2010. [Online]. Available: https://doi.org/10.1016/j.corsci.2010.06.003

[80] A. Abdal-hay, M. Dewidar, J. Lim, and J. K. Lim, "Enhanced biocorrosion resistance of surface modified magnesium alloys using inorganic/organic composite layer for biomedical applications," *Ceramics International*, vol. 40, no. 1, Aug. 06, 2013. [Online]. Available: https://doi.org/10.1016/j.ceramint.2013.07.142

[81] Z. Chun-Yan, Z. Rong-Chang, L. Cheng-Long, and G. Jiao-Cheng, "Comparison of calcium phosphate coatings on mg–al and mg–ca alloys and their corrosion behavior in hank's solution," *Surface and Coatings Technology*, vol. 204, no. 21-22, Apr. 18, 2010. [Online]. Available: https://doi.org/10.1016/j.surfcoat.2010.04.038

[82] S. Fajardo and G. S. Frankel, "Gravimetric method for hydrogen evolution measurements on dissolving magnesium," *Journal of The Electrochemical Society*, vol. 162, no. 14, Sep. 25, 2015. [Online]. Available: https://doi.org/10.1149/2.0241514jes

[83] S. Lebouil, A. Duboin, F. Monti, P. Tabeling, P. Volovitch, and *et al.*, "A novel approach to on-line measurement of gas evolution kinetics: Application to the negative difference effect of mg in chloride solution," *Electrochimica Acta*, vol. 124, Jul. 31, 2013. [Online]. Available: https://doi.org/10.1016/j.electacta.2013.07.131

[84] A. D. King, N. Birbilis, and J. R. Scully, "Accurate electrochemical measurement of magnesium corrosion rates; a combined impedance, mass-loss and hydrogen collection study," *Electrochimica Acta*, vol. 121, Jan. 04, 2014. [Online]. Available: https://doi.org/10.1016/j.electacta.2013.12.124

[85] Y. Jang, Z. Tan, C. Jurey, B. Collins, A. Badve, and *et al.*, "Systematic understanding of corrosion behavior of plasma electrolytic oxidation treated az31 magnesium alloy using a mouse model of subcutaneous implant," *Materials Science and Engineering: C*, vol. 45, Sep. 06, 2014. [Online]. Available: https://doi.org/10.1016/j.msec.2014.08.052

[86] S. Feliu-Jr, "Electrochemical impedance spectroscopy for the measurement of the corrosion rate of magnesium alloys: Brief review and challenges," *Metals*, vol. 10, no. 6, Jun. 10, 2020. [Online]. Available: https://doi.org/10.3390/met10060775

[87] C. Wang, B. Jiang, M. Liu, and Y. Ge, "Corrosion characterization of micro-arc oxidization composite electrophoretic coating on az31b magnesium alloy," *Journal of Alloys and Compounds*, vol. 621, Oct. 05, 2014. [Online]. Available: https://doi.org/10.1016/j.jallcom.2014.09.168

[88] L. Wolters, S. Besdo, N. Angrisani, P. Wriggers, B. Hering, and *et al.*, "Degradation behaviour of lae442-based plate–screw-systems in an in vitro bone model," *Materials Science and Engineering: C*, vol. 49, Jan. 07, 2015. [Online]. Available: https://doi.org/10.1016/j.msec.2015.01.019

[89] H.-S. Hang, Y. Minghui, H.-K. Seok, J.-Y. Byun, P.-R. Cha, and *et al.*, "The modification of microstructure to improve the biodegradation and mechanical properties of a biodegradable mg alloy," *Journal of the Mechanical Behavior of Biomedical Materials*, vol. 20, Dec. 28, 2012. [Online]. Available: https://doi.org/10.1016/j.jmbbm.2012.12.007

[90] A. Zakiyudding and K. Lee, "Effect of a small addition of zinc and manganese to mg–ca based alloys on degradation behavior in physiological media," *Journal of Alloys and Compounds*, vol. 629, Dec. 31, 2014. [Online]. Available: https://doi.org/10.1016/j.jallcom.2014.12.181

[91] M. Echeverry-Rendón, L. F. Berrio, S. M. Robledo, J. A. Calderón, J. G. Castaño, and *et al.*, "Corrosion resistance and biological properties of pure magnesium modified by peo in alkaline phosphate solutions," *Corrosion and Materials Degradation*, vol. 4, no. 2, Mar. 23, 2023. [Online]. Available: https://doi.org/10.3390/cmd4020012

[92] X. N. Gu, N. Li, W. R. Zhou, Y. F. Zheng, X. Zhao, and *et al.*, "Corrosion resistance and surface biocompatibility of a microarc oxidation coating on a mg–ca alloy," *Acta Biomaterialia*, vol. 7, no. 4, Dec. 08, 2010. [Online]. Available: https://doi.org/10.1016/j.actbio.2010.11.034

[93] S. Gaur, R. K. Singh-Raman, and A. S. Khanna, "*In vitro* investigation of biodegradable polymeric coating for corrosion resistance of mg-6zn-ca alloy in simulated body fluid," *Materials Science and Engineering: C*, vol. 42, May. 22, 2014. [Online]. Available: https://doi.org/10.1016/j.msec.2014.05.035

[94] Q. Sun, J. Yang, R. Tian, X. Fan, Z. Liao, and *et al.*, "Enhanced corrosion and wear resistances in a precipitate-hardened magnesium alloy by laser surface remelting," *Materials Characterization*, vol. 193, Sep. 15, 2022. [Online]. Available: https://doi.org/10.1016/j.matchar.2022.112306

[95] H. Liu, J. Gu, Z. Tong, D. Yang, H. Yang, and *et al.*, "Improving stress corrosion cracking resistance of az31 magnesium alloy in hanks' solution via phosphate conversion with laser shock peening pretreatment," *Materials Today Communications*, vol. 31, May. 13, 2022. [Online]. Available: https://doi.org/10.1016/j.mtcomm.2022.103678

[96] D. B. Pokharel, L. Wu, J. Dong, A. P. Yadav, D. B. Subedi, and *et al.*, "Effect of glycine addition on the in-vitro corrosion behavior of az31 magnesium alloy in hank's solution," *Journal of Materials Science & Technology*, vol. 81, Jan. 05, 2021. [Online]. Available: https://doi.org/10.1016/j.jmst.2021.01.007

[97] J. da Silva-Rodríguez, L. Marasca-Antonini, A. A. D. C. Bastos, J. Zhou, and C. de Fraga-Malfatti, "Corrosion resistance and tribological behavior of zk30 magnesium alloy coated by plasma electrolytic oxidation," *Surface and Coatings Technology*, vol. 410, Feb. 19, 2021. [Online]. Available: https://doi.org/10.1016/j.surfcoat.2021.126983

[98] J. Dou, J. Wang, H. Li, Y. Lu, H. Yu, and *et al.*, "Enhanced corrosion resistance of magnesium alloy by plasma electrolytic oxidation plus hydrothermal treatment," *Surface and Coatings Technology*, vol. 424, Sep. 03, 2021. [Online]. Available: https://doi.org/10.1016/j.surfcoat.2021.127662

[99] H. S. Brar, I. S. Berglund, J. B. Allen, and M. V. Manuel, "The role of surface oxidation on the degradation behavior of biodegradable mg–re (gd, y, sc) alloys for resorbable implants," *Materials Science and Engineering: C*, vol. 40, Mar. 30, 2014. [Online]. Available: https://doi.org/10.1016/j.msec.2014.03.055

[100] R.-C. Zeng, Y. Hu, S.-K. Guan, H.-Z. Cui, and E.-H. Han, "Corrosion of magnesium alloy az31: The influence of bicarbonate, sulphate, hydrogen phosphate and dihydrogen phosphate ions in saline solution," *Corrosion Science*, vol. 86, May. 13, 2014. [Online]. Available: https://doi.org/10.1016/j.corsci.2014.05.006

[101] D. Zander and N. Z. Zumdick, "Influence of ca and zn on the microstructure and corrosion of biodegradable mg–ca–zn alloys," *Corrosion Science*, vol. 93, Jan. 21, 2015. [Online]. Available: https://doi.org/10.1016/j.corsci.2015.01.027

[102] G. G. Perrault, "The potential-ph diagram of the magnesium-water system," *Journal of Electroanalytical Chemistry and Interfacial Electrochemistry*, vol. 51, no. 1, Dec. 02, 2010. [Online]. Available: https://doi.org/10.1016/S0022-0728(74)80298-6

[103] J. Jiang, F. Zhang, A. Ma, D. Song, J. Chen, and *et al.*, "Biodegradable behaviors of ultrafine-grained ze41a magnesium alloy in dmem solution," *Metals*, vol. 6, no. 1, Dec. 23, 2015. [Online]. Available: https://doi.org/10.3390/met6010003

[104] M.-C. Zhao, M. Liu, G.-L. Song, and A. Atrens, "Influence of ph and chloride ion concentration on the corrosion of mg alloy ze41," *Corrosion Science*, vol. 50, no. 11, Aug. 26, 2008. [Online]. Available: https://doi.org/10.1016/j.corsci.2008.08.023

[105] N.-G. Wang, R.-C. Wang, C.-Q. Peng, Y. Feng, and X.-Y. Zhang, "Corrosion behavior of mg-al-pb and mg-al-pb-zn-mn alloys in 3.5*Transactions of Nonferrous Metals Society of China*, vol. 20, no. 10, Nov. 07, 2010. [Online]. Available: https://doi.org/10.1016/S1003-6326(09)60398-8

[106] Z. Shi, J. X. Jia, and A. Atrens, "Galvanostatic anodic polarisation curves and galvanic corrosion of high purity mg in 3.5mg(oh)$_2$," *Corrosion Science*, vol. 60, Dec. 14, 2011. [Online]. Available: https://doi.org/10.1016/j.corsci.2011.12.002

[107] T. Watanabe, Y. C. Huang, and R. Komatsu, "Solubility of hydrogen in magnesium," *Journal of Japan Institute of Light Metals*, vol. 26, no. 2, 1976. [Online]. Available: https://doi.org/10.2464/jilm.26.76

[108] J. D. Shearouse and B. A. Mikucki, "The origin of microporosity in magnesium alloy az91," SAE International, United States, Tech. Rep. 940776, Mar. 01, 1994. [Online]. Available: https://doi.org/10.4271/940776

[109] M. Kappes, M. Lannuzzi, and R. M. Carranza, "Hydrogen embrittlement of magnesium and magnesium alloys: A review," *Journal of The Electrochemical Society*, vol. 160, no. 4, Feb. 26 2013. [Online]. Available: https://doi.org/10.1149/2.023304jes

[110] S. V. Lamaka, B. Vaghefinazari, D. Mei, R. P. Petrauskas, and D. Höche, "Comprehensive screening of mg corrosion inhibitors," *Corrosion Science*, vol. 128, Jul. 25, 2017. [Online]. Available: https://doi.org/10.1016/j.corsci.2017.07.011

[111] W.-D. Mueller, "Electrochemical techniques for assessment of corrosion behaviour of mg and mg-alloys," *BioNanoMaterials*, vol. 16, no. 1, May. 26, 2015. [Online]. Available: https://doi.org/10.1515/bnm-2015-0006

[112] D. Xue, Y. Yun, M. J. Schulz, and V. Shanov, "Corrosion protection of biodegradable magnesium implants using anodization," *Materials Science and Engineering: C*, vol. 31, no. 2, Aug. 25, 2010. [Online]. Available: https://doi.org/10.1016/j.msec.2010.08.019

[113] M. E. Straumanis and B. K. Bhatia, "Disintegration of magnesium while dissolving anodically in neutral and acidic solutions," *Journal of The Electrochemical Society*, vol. 110, no. 5, 1963. [Online]. Available: https://doi.org/10.1149/1.2425763

[114] C. R. Weber, G. Knörnschild, and L. F. P. Dick, "The negative-difference effect during the localized corrosion of magnesium and of the az91hp alloy," *Journal of the Brazilian Chemical Society*, vol. 14, no. 4, Aug. 2003. [Online]. Available: https://doi.org/10.1590/S0103-50532003000400015

[115] Z. Shi, M. Liu, and A. Atrens, "Measurement of the corrosion rate of magnesium alloys using tafel extrapolation," *Corrosion Science*, vol. 52, no. 2, Oct. 15, 2009. [Online]. Available: https://doi.org/10.1016/j.corsci.2009.10.016

[116] R. L. Petty, A. W. Davidson, and J. Kleinberg, "The anodic oxidation of magnesium metal: Evidence for the existence of unipositive magnesium," *Journal of American Chemical Society*, vol. 76, no. 2, Jan. 01, 1954. [Online]. Available: https://doi.org/10.1021/ja01631a013

[117] G. Song and A. Atrens, "Understanding magnesium corrosion—a framework for improved alloy performance," *Advanced Engineering Materials*, vol. 5, no. 12, Jan. 08, 2004. [Online]. Available: https://doi.org/10.1002/adem.200310405

[118] C. Liu, J. Liang, J. Zhou, L. Wang, and Q. Li, "Effect of laser surface melting on microstructure and corrosion characteristics of am60b magnesium alloy," *Applied Surface Science*, vol. 343, Mar. 20, 2015. [Online]. Available: https://doi.org/10.1016/j.apsusc.2015.03.067

[119] M. I. Jamesh, G. Wu, Y. Zhao, D. R. Mckenzie, M. M. M. Bilek, and *et al.*, "Effects of zirconium and oxygen plasma ion implantation on the corrosion behavior of zk60 mg alloy in simulated body fluids," *Corrosion Science*, vol. 82, Dec. 04, 2013. [Online]. Available: https://doi.org/10.1016/j.corsci.2013.11.044

[120] X.-B. Liu, D. Shan, Y.-W. Song, and E.-H. Han, "Effects of heat treatment on corrosion behaviors of mg-3zn magnesium alloy," *Transactions of Nonferrous Metals Society of China*, vol. 20, no. 7, Aug. 10, 2010. [Online]. Available: https://doi.org/10.1016/S1003-6326(09)60302-2

[121] T. Mi, B. Jiang, Z. Liu, and L. Fan, "Plasma formation mechanism of microarc oxidation," *Electrochimica Acta*, vol. 123, no. 7, Jan. 23, 2014. [Online]. Available: https://doi.org/10.1016/j.electacta.2014.01.047

[122] D. Veys-Renaux, C.-E. Barchiche, and E. Rocca, "Corrosion behavior of az91 mg alloy anodized by low-energy micro-arc oxidation: Effect of aluminates and silicates," *Surface and Coatings Technology*, vol. 251, Apr. 26, 2014. [Online]. Available: https://doi.org/10.1016/j.surfcoat.2014.04.031

[123] L. Zhao, C. Cui, and Q. W. S. Bu, "Growth characteristics and corrosion resistance of micro-arc oxidation coating on pure magnesium for biomedical applications," *Corrosion Science*, vol. 52, no. 7, Mar. 15, 2010. [Online]. Available: https://doi.org/10.1016/j.corsci.2010.03.008

[124] T. Zhao, Z. Wang, Y. Feng, and Q. Li, "Synergistic corrosion inhibition of sodium phosphate and sodium dodecyl sulphate on magnesium alloy az91 in 3.5 wt2022. [Online]. Available: https://doi.org/10.1016/j.mtcomm.2022.103568

[125] H. R. Bakhsheshi-Rad, M. H. Idris, M. R. Abdul-Kadir, A. Ourdjini, M. Medraj, and *et al.*, "Mechanical and bio-corrosion properties of quaternary mg–ca–mn–zn alloys compared with binary mg–ca alloys," *Materials & Design*, vol. 53, Jul. 03, 2013. [Online]. Available: https://doi.org/10.1016/j.matdes.2013.06.055

[126] D. S. A. Ma, J. Jiang, P. Lin, D. Yang, and J. Fan, "Corrosion behavior of equal-channel-angular-pressed pure magnesium in nacl aqueous solution," *Corrosion Science*, vol. 52, no. 2, Oct. 13, 2009. [Online]. Available: https://doi.org/10.1016/j.corsci.2009.10.004

[127] K. C. Tekin, U. Malayoğlu, and S. Shrestha, "Electrochemical behavior of plasma electrolytic oxide coatings on rare earth element containing mg alloys," *Surface and Coatings Technology*, vol. 236, Oct. 31, 2013. [Online]. Available: https://doi.org/10.1016/j.surfcoat.2013.10.051

[128] L. Li, Z. Huang, L. Chen, L. Zhang, M. Li, and *et al.*, "Electrochemical corrosion behavior of az91d magnesium alloy-graphene nanoplatelets composites in simulated body fluids," *Journal of Materials Research and Technology*, vol. 24, Mar. 08, 2023. [Online]. Available: https://doi.org/10.1016/j.jmrt.2023.01.232

[129] P. B. Srinivasan, J. Liang, C. Blawert, M. Störmer, and W. Dietzel, "Characterization of calcium containing plasma electrolytic oxidation coatings on am50 magnesium alloy," *Applied Surface Science*, vol. 256, no. 12, Jan. 29, 2010. [Online]. Available: https://doi.org/10.1016/j.apsusc.2010.01.069

[130] C. Hu, Q. Le, X. Zhou, C. Cheng, R. Guo, X. Li, and *et al.*, "The growth and corrosion mechanism of zn-based coating on az31 magnesium alloys by novel hot-dip process," *Materials Characterization*, vol. 189, May. 18, 2022. [Online]. Available: https://doi.org/10.1016/j.matchar.2022.111988

[131] D. Sreekanth, N. Rameshbabu, and K. Venkateswarlu, "Effect of various additives on morphology and corrosion behavior of ceramic coatings developed on az31 magnesium alloy by plasma electrolytic oxidation," *Ceramics International*, vol. 38, no. 6, Feb. 21, 2012. [Online]. Available: https://doi.org/10.1016/j.ceramint.2012.02.040

[132] H. Du, Z. Wei, H. Wang, E. Zhang, L. Zuo, and *et al.*, "Surface microstructure and cell compatibility of calcium silicate and calcium phosphate composite coatings on mg–zn–mn–ca alloys

for biomedical application," *Colloids and Surfaces B: Biointerfaces*, vol. 83, no. 1, Nov. 09, 2010. [Online]. Available: https://doi.org/10.1016/j.colsurfb.2010.11.003

[133] B. N. Grgur, B. Z. Jugovic, and M. M. Gvozdenovic, "Influence of chloride ion concentration on initial corrosion of az63 magnesium alloy," *Transactions of Nonferrous Metals Society of China*, vol. 32, no. 4, May 12, 2022. [Online]. Available: https://doi.org/10.1016/S1003-6326(22)65861-8

[134] J. Zhang, S. Hiromoto, T. Yamazaki, J. Niu, H. Huang, G. Jia, and *et al.*, "Effect of macrophages on in vitro corrosion behavior of magnesium alloy," *Journal of Biomedical Materials Research Part A*, vol. 104, no. 10, May. 25, 2016. [Online]. Available: https://doi.org/10.1002/jbm.a.35788

[135] Q. Peng, H. Fu, J. Pang, J. Zhang, and W. Xiao, "Preparation, mechanical and degradation properties of mg–y-based microwire," *Journal of the Mechanical Behavior of Biomedical Materials*, vol. 29, Oct. 12, 2013. [Online]. Available: https://doi.org/10.1016/j.jmbbm.2013.09.015

[136] M. I. James, G. Wu, Y. Zhao, D. R. Mckenzie, M. M. M. Bilek, and *et al.*, "Electrochemical corrosion behavior of biodegradable mg–y–re and mg–zn–zr alloys in ringer's solution and simulated body fluid," *Corrosion Science*, vol. 91, Nov. 15, 2014. [Online]. Available: https://doi.org/10.1016/j.corsci.2014.11.015

[137] L.-Y. Cui, Y. Hu, R.-C. Zeng, Y.-X. Yang, D.-D. Sun, and *et al.*, "New insights into the effect of tris-hcl and tris on corrosion of magnesium alloy in presence of bicarbonate, sulfate, hydrogen phosphate and dihydrogen phosphate ions," *Journal of Materials Science & Technology*, vol. 33, no. 9, Jan. 07, 2017. [Online]. Available: https://doi.org/10.1016/j.jmst.2017.01.005

[138] N. Dinodi and A. N. Shetty, "Electrochemical investigations on the corrosion behaviour of magnesium alloy ze41 in a combined medium of chloride and sulphate," *Journal of Magnesium and Alloys*, vol. 1, no. 3, Sep. 15, 2013. [Online]. Available: https://doi.org/10.1016/j.jma.2013.08.003

[139] R. O. Hussein, D. O. Northwood, and X. Nie, "The effect of processing parameters and substrate composition on the corrosion resistance of plasma electrolytic oxidation (peo) coated magnesium alloys," *Surface and Coatings Technology*, vol. 237, Sep. 18, 2013. [Online]. Available: https://doi.org/10.1016/j.surfcoat.2013.09.021

[140] S. A. Bacha, I. Aubert, O. Devos, M. Zakhour, M. Nakhl, and *et al.*, "Corrosion of pure and milled $mg_{17}al_{12}$ in "model" seawater solution," *International Journal of Hydrogen Energy*, vol. 45, no. 32, May. 01, 2020. [Online]. Available: https://doi.org/10.1016/j.ijhydene.2020.04.030

[141] M. Ascencio, M. Pekguleryuz, and S. Omanovic, "An investigation of the corrosion mechanisms of we43 mg alloy in a modified simulated body fluid solution: The influence of immersion time," *Corrosion Science*, vol. 87, Jul. 16, 2014. [Online]. Available: https://doi.org/10.1016/j.corsci.2014.07.015

[142] M. Pereira-Gomes, I. Costa, and N. Pébère, "On the corrosion mechanism of mg investigated by electrochemical impedance spectroscopy," *Electrochimica Acta*, vol. 306, Mar. 14, 2019. [Online]. Available: https://doi.org/10.1016/j.electacta.2019.03.080

[143] A. Doepke, J. Kuhlmann, X. Guo, R. T. Voorhees, and W. R. Heineman, "A system for characterizing mg corrosion in aqueous solutions using electrochemical sensors and impedance spectroscopy," *Acta Biomaterialia*, vol. 9, no. 11, Jul. 18, 2013. [Online]. Available: https://doi.org/10.1016/j.actbio.2013.07.011

[144] L. S. K. Leinartas, E. Juzeliūnas, D. B. A. Grigucevičienė, and *et al.*, "Anticorrosion performance of hafnium oxide ultrathin films on az31 magnesium alloy," *Surface and Coatings Technology*, vol. 397, Jun. 09, 2020. [Online]. Available: https://doi.org/10.1016/j.surfcoat.2020.126046

[145] K. Dorado-Bustamante, B. Zuluaga-Díaz, and H. Estupiñán-Duran, "Análisis de la bioactividad de mg az31 recubierta por peo (plasma electrolytic oxidation)," *DYNA*, vol. 85, no. 205, Apr. 01, 2018. [Online]. Available: https://doi.org/10.15446/dyna.v85n205.69573

[146] M. Curioni, F. Scenini, T. monetta, and F. Bellucci, "Correlation between electrochemical impedance measurements and corrosion rate of magnesium investigated by real-time hydrogen measurement and optical imaging," *Electrochimica Acta*, vol. 166, Mar. 11, 2015. [Online]. Available: https://doi.org/10.1016/j.electacta.2015.03.050

[147] E. Bütev-Öcal, Z. Esen, K. Aydinol, and A. F. Dericioğlu, "Comparison of the short and long-term degradation behaviors of as-cast pure mg, az91 and we43 alloys," *Materials Chemistry and Physics*, vol. 241, Oct. 23, 2019. [Online]. Available: https://doi.org/10.1016/j.matchemphys.2019.122350

[148] Y. Liu, M. Curioni, and Z. Liu, "Correlation between electrochemical impedance measurements and corrosion rates of mg-1ca alloy in simulated body fluid," *Electrochimica Acta*, vol. 264, Feb. 06, 2018. [Online]. Available: https://doi.org/10.1016/j.electacta.2018.01.121

[149] W. Aperador-Chaparro, G. Rodríguez-Zamora, and F. Franco-Arenas, "Estimación de la corrosión intergranular en la aleación de magnesio az31b soldada por fricción - agitación," *Revista de Ingeniería*, no. 39, Jun-Dec. 2013. [Online]. Available: http://www.scielo.org.co/scielo.php?pid=S0121-49932013000200007&script=sci_arttext

[150] A. Atrens, Z. Shi, S. U. Mehreen, S. Johnston, G.-L. Song, and *et al.*, "Review of mg alloy corrosion rates," *Journal of Magnesium and Alloys*, vol. 8, no. 4, Sep. 28, 2020. [Online]. Available: https://doi.org/10.1016/j.jma.2020.08.002

[151] A. Atrens, G.-L. Song, F. Cao, Z. Shi, and P. K. Bowen, "Advances in mg corrosion and research suggestions," *Journal of Magnesium and Alloys*, vol. 1, no. 3, Oct. 10, 2013. [Online]. Available: https://doi.org/10.1016/j.jma.2013.09.003

[152] M. Esmaily, J. E. Svensson, S. Fajardo, N. Birbilis, G. S. Frankel, and *et al.*, "Fundamentals and advances in magnesium alloy corrosion," *Progress in Materials Science*, vol. 89, May. 15, 2017. [Online]. Available: https://doi.org/10.1016/j.pmatsci.2017.04.011

[153] A. Atrens, S. Johnston, Z. Shi, and M. S. Dargusch, "Viewpoint - understanding mg corrosion in the body for biodegradable medical implants," *Scripta Materialia*, vol. 154, May. 30, 2018. [Online]. Available: https://doi.org/10.1016/j.scriptamat.2018.05.021

[154] A. Atrens, S. Johnston, Z. Shi, and M. s. Dargusch, "Real-time monitoring of atmospheric magnesium alloy corrosion," *Journal of The Electrochemical Society*, vol. 166, no. 11, Dec. 12, 2018. [Online]. Available: https://doi.org/10.1149/2.0011911jes